CMLS, Cell. Mol. Life Sci. 57 (2000) 1236–1259
1420-682X/00/091236-24 $ 1.50 + 0.20/0

CMLS Cellular and Molecular Life Sciences

Review

New insights into copper monooxygenases and peptide amidation: structure, mechanism and function

S. T. Prigge[a], R. E. Mains[b], B. A. Eipper[b,1] and L. M. Amzel[a,*,†]

[a]Department of Biophysics and Biophysical Chemistry, The Johns Hopkins University School of Medicine, 725 N. Wolfe Street, Baltimore (Maryland 21205, USA)
[b]Departments of Neuroscience and Physiology, The Johns Hopkins University School of Medicine, 725 N. Wolfe Street, Baltimore (Maryland 21205, USA)

Received 7 December 1999; received after revision 24 February 2000; accepted 29 February 2000

Abstract. Many bioactive peptides must be amidated at their carboxy terminus to exhibit full activity. Surprisingly, the amides are not generated by a transamidation reaction. Instead, the hormones are synthesized from glycine-extended intermediates that are transformed into active amidated hormones by oxidative cleavage of the glycine N-Cα bond. In higher organisms, this reaction is catalyzed by a single bifunctional enzyme, peptidylglycine α-amidating monooxygenase (PAM). The PAM gene encodes one polypeptide with two enzymes that catalyze the two sequential reactions required for amidation. Peptidylglycine α-hydroxylating monooxygenase (PHM; EC 1.14.17.3) catalyzes the stereospecific hydroxylation of the glycine α-carbon of all the peptidylglycine substrates. The second enzyme, peptidyl-α-hydroxyglycine α-amidating lyase (PAL; EC 4.3.2.5), generates α-amidated peptide product and glyoxylate. PHM contains two redox-active copper atoms that, after reduction by ascorbate, catalyze the reduction of molecular oxygen for the hydroxylation of glycine-extended substrates. The structure of the catalytic core of rat PHM at atomic resolution provides a framework for understanding the broad substrate specificity of PHM, identifying residues critical for PHM activity, and proposing mechanisms for the chemical and electron-transfer steps in catalysis. Since PHM is homologous in sequence and mechanism to dopamine β-monooxygenase (DBM; EC 1.14.17.1), the enzyme that converts dopamine to norepinephrine during catecholamine biosynthesis, these structural and mechanistic insights are extended to DBM.

Key words. Amidation; copper; peptidylglycine α-amidating monooxygenase; dopamine β-monooxygenase; electron transfer; structure; ascorbate; peptide hormones; oxygen chemistry.

Introduction

Peptide amidation is a ubiquitous posttranslational modification of bioactive peptides. Over half of all peptide hormones require amidation to achieve full biological activity. The amidation reaction is catalyzed by two enzymes: peptidylglycine α-hydroxylating monooxygenase (PHM; EC 1.14.17.3) and peptidyl-α-hydroxyglycine α-amidating lyase (PAL; EC 4.3.2.5). In some organisms these enzymes are expressed independently, whereas in higher organisms both are expressed on one polypeptide chain. These enzymes can produce amides of all 20 amino acids as well as fatty acyl amides. The first half of this review focuses on the biology of these enzymes and the role of the amidated

* Corresponding author.
† BEA (beipper@jhmi.edu) and LMA (mamzel@jhmi.edu) are equally contributing senior authors.

peptides that they produce. The latter half focuses on the structure and mechanism of PHM and how these insights apply to related enzymes.

Peptide amidation and the bifunctional PAM protein: PHM and PAL

Bioactive peptides are important as hormones, neurotransmitters and paracrine agents. Most bioactive peptides are synthesized from large, inactive precursors by a set of co- and posttranslational modifications including signal peptide cleavage, disulfide bond formation, addition of N-and O-linked oligosaccharide chains and endoproteolysis [1–8]. Over half of these peptides require formation of a C-terminal α-amide to gain full biological activity [9, 10]. Peptidylglycine α-amidating monooxygenase (PAM; EC 1.14.17.3), a bifunctional enzyme, catalyses the conversion of peptidylglycine substrates into α-amidated products in a two step reaction (fig. 1, top). The first step of the amidation reaction is catalyzed by PHM, whereas the second step is catalyzed by PAL. PAM is the only enzyme known to be capable of catalyzing the formation of amidated peptides; genetic deletion of the *Drosophila* enzyme eliminates production of amidated peptides and results in early embryonic lethality [11].

The structure of the bifunctional PAM protein is similar in many species [12] (fig. 1, bottom). The PAM protein has an NH_2-terminal signal sequence, followed by a short proregion that is cleaved from PHM proteins isolated from bovine pituitary and frog skin. The PAL enzyme is located C-terminal to the PHM enzyme, separated from PHM by a noncatalytic segment called exon A that can be excluded as a result of alternative splicing. The PAL enzyme is followed by a transmembrane domain and a short C-terminal domain. PHM and PAL can be expressed independently or generated by endoproteolytic cleavage of PAM. The PHM enzyme is an ascorbate-dependent, colorless monooxygenase containing two coppers [13, 14] that cycle between Cu^+ and Cu^{2+} during the monooxygenase reaction [15]. These copper atoms are easily removed with chelators and completely restored by addition of cupric ion [12, 14]. PHM activity is not supported by metals other than copper. Several agents

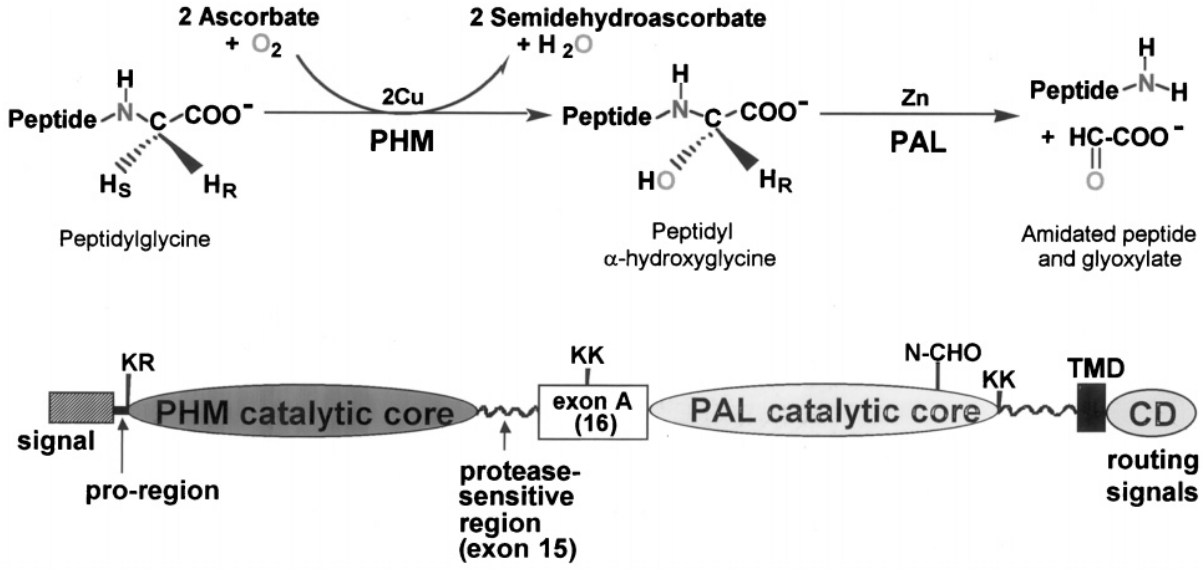

Figure 1. The PAM Reaction and the PAM Protein. (Top) The two-step conversion of peptidylglycine substrates into products is shown. Peptidylglycine α-hydroxylating monooxygenase, PHM, has also been referred to as peptidylglycine α-amidating monooxygenase and peptidylglycine hydroxylase; peptidyl-α-hydroxyglycine α-amidating lyase, PAL, has also been referred to as peptidylamidoglycolate lyase and peptidyl-α-hydroxyglycine lyase. (Bottom) The structure of a bifunctional membrane PAM protein that includes exon A (exon 16) is shown. The hydrophobic signal sequence is removed in the endoplasmic reticulum. The 10-residue proregion is removed in a post-Golgi compartment in neuroendocrine cells; its presence facilitates exit from the endoplasmic reticulum but does not affect catalytic activity. A protease-sensitive region (exon 15) separates the end of the PHM catalytic core from exon A [121]. Tissue-specific endoproteoytic cleavage in exon A can generate soluble PHM and membrane PAL. The PAL enzyme contains a single N-glycosylation site (N-CHO) and terminates just before Lys821-Lys822. Endoproteolytic cleavage can occur between PAL and the transmembrane domain (TMD), but the cleavage sites are not well characterized. The cytosolic region (cytosolic domain, CD) contains signals important to the localization of PAM in the distal trans-Golgi network and to its endocytosis from the plasma membrane [110].

can reduce the two PHM copper atoms from Cu^{2+} to Cu^{+} through two single-electron transfers; however, reactions using ascorbic acid as the reductant result in the highest PHM activity in test-tube assays and in cultured cells [16–21]. One mole of ascorbic acid is consumed for each mole of amidated product [17]. Soluble, bifunctional PAM contains a single zinc atom which may be bound to the PAL enzyme [22]. The enzymatic activity of PAL is abolished by chelators such as EDTA, but in contrast to the metal specificity of PHM, PAL activity can be restored with a slight molar excess of several divalent metal ions [12].

Amidated peptides: ancient and broadly expressed messengers

Peptides terminating with an α-amide are found widely in vertebrates and invertebrates; examples include substance P, neuropeptide Y, oxytocin and vasopressin, gastrin, calcitonin, many of the snail conotoxins, locust adipokinetic hormone, *Aplysia* egg-laying hormone and many of the antimicrobial peptides isolated from the hemolymph of shrimp (reviewed in [14, 23–27]). Although α-amidation does not occur in yeast, an amidated peptide, pyro-Glu-Tyr-Pro-NH_2, has been isolated from dried alfalfa pellets [28]. It seems safe to assume that complementary DNAs (cDNAs) encoding secretory products that can be cleaved to yield a peptide with a C-terminal Gly will generate an α-amidated product when expressed in tissues producing PAM.

For most α-amidated peptides, the α-amide group is required for full biological activity. By preventing ionization of the C-terminus, α-amidation may render a peptide more hydrophobic and thus better able to bind to its receptor. Studies on the interaction of a variety of G-protein-coupled peptide receptors with their amidated peptide ligands show the amide moiety as a key determinant of interaction with the receptor [29–31]. At least one amidated tetrapeptide, Phe-Met-Arg-Phe-NH_2 or FMRF-NH_2, activates an amiloride-sensitive Na^{+} channel, the first peptide-gated ionotropic receptor [32]. In general, glycine-extended peptides are not prevalent in tissue extracts and act as transient intermediates in the biosynthetic pathway leading to amidated products [33]. However, gastrin-Gly [34–36], adrenomedullin-Gly [37] and oxytocin-Gly [38] are major forms in the circulation. Gastrin-Gly, acting through a receptor distinct from the receptor for gastrin-NH_2, has its own unique biological effects [34, 35, 39, 40]. In cases where both the Gly-extended precursor and amidated product have distinct biological activities, control of amidation is of special importance.

Primitive organisms such as the *Cnidarians* (sea anemone, *Hydra*), which have an organized nerve net, produce a variety of amidated peptides, and lack classical transmitters such as acetylcholine and catecholamines [41]. It is estimated that *Hydra* contain over 1300 peptides, many of which are amidated [26]. In *Hydra* these peptide precursors are expressed in strictly controlled spatial and temporal patterns [42] and regulate functions such as muscle contraction and induction of metamorphosis [24, 43].

The role of amidated peptides as frequency-dependent, neuromodulatory cotransmitters has been best defined in *Aplysia* [44, 45]. In *Caenorhabditis elegans*, over 18 genes encode more than 53 FMRF-NH_2-related peptides. Despite this apparent redundancy, disruption of a single FMRF-NH_2 precursor gene leads to uncoordinated movements, hyperactivity and insensitivity to high osmolarity [46].

Consistent with their ancient use as signaling molecules, amidated peptides are involved in a diverse array of functions in vertebrate systems. Early structure/function studies demonstrated the importance of amidation to peptide hormones that are made and stored in classical endocrine tissues (e.g. vasopressin, gastrin and gonadotropin-releasing hormone). It is now clear that amidated peptides are expressed in a wide variety of tissues and used as paracrine and autocrine factors. For example, adrenomedullin is a hypotensive peptide produced in endothelial cells, chondrocytes and vascular smooth muscle cells [47, 48]. Pituitary adenylate cyclase-activating peptide (PACAP) increases the survival of sensory and motor neurons during embryonic development [49], and substance P may play a role in axon guidance [50].

PAM substrates

The ability of PAM to produce peptides terminating with all 20 amino acid amides has been appreciated for some time [10, 23]. Interestingly, substrates terminating in D-amino acids can also be PAM substrates. When mammalian cells were engineered to produce gastrin with its C-terminal Gly substituted with Ser or Ala, no amidation occurred; after feeding the cells D-Ser or D-Ala, a small amount of amidated gastrin was detected [51]. Landymore-Lim and co-workers [52] showed that peptides ending in D-Ala were indeed substrates for PAM. Early studies indicated that purified PHM could also catalyze N-dealkylation, O-dealkylation and sulfoxidation reactions of nonpeptide substrates (fig. 2A) [53]. More recent studies indicate that PAM can accommodate a wide variety of nonpeptide substrates [14, 54–56]. Purified recombinant PAM efficiently converts fatty acyl glycines, ranging in length from N-formyl to N-arachidonyl, into fatty acyl amides through an N-acyl-α-hydroxyglycine intermediate (fig. 2B). Thus PAM may produce oleamide, a fatty acyl amide iden-

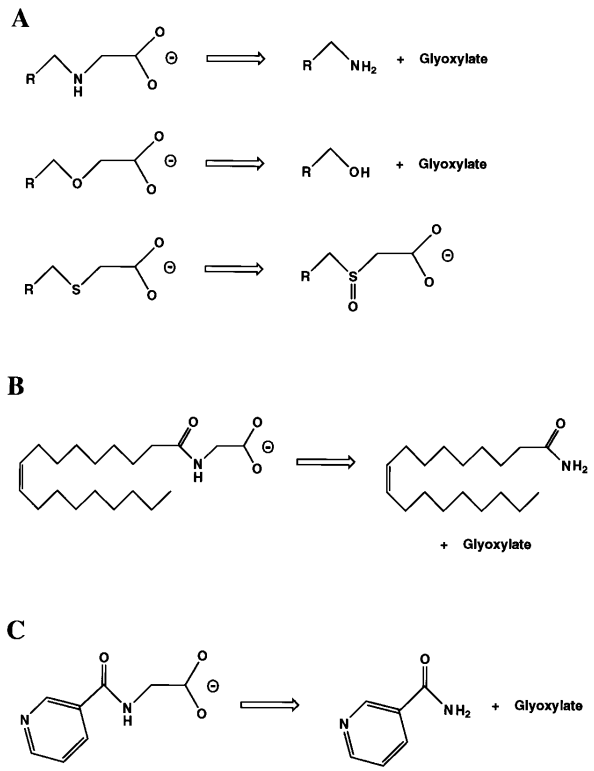

Figure 2. Diversity of Substrates/Reactions Accommodated by PAM. (*A*) A variety of potential nonpeptide substrates were tested with monofunctional PHM purified from frozen bovine pituitaries. N-dealkylation, O-dealkylation and sulfoxidation reactions are shown [53]. (*B*) PAM catalyzes the oxidative cleavage of N-acylglycines ranging in length from N-formyl to N-arachidonyl [54, 55]; the formation of oleamide, a potent sleep-inducing agent, is shown [57, 58]. (*C*) PAM converts nicotinuric acid into nicotinamide via a hydroxyglycine intermediate, suggesting a role for PAM in the formation of many nonpeptide primary amides [56].

tified in the cerebrospinal fluid of sleep-deprived cats; upon injection into rats, oleamide induces physiological sleep and modulates serotonergic signal transduction [57, 58]. PAM also catalyzes the conversion of nicotinuric acid into nicotinamide [56] (fig. 2C). Access of potential substrates to PAM is clearly critical in determining which of the reactions are catalyzed in vivo.

Sites of expression of PAM

In the adult, expression of PAM is highest in atrial myocytes, endocrine cells of the pituitary and in many neurons. However, PAM expression is not limited to classical neuroendocrine tissues. PAM is found in airway and olfactory epithelium, endothelial cells, chondrocytes of bronchial cartilage, smooth muscle cells, brain ependymal cells and astrocytes [12, 59–63].

During development, PAM appears first in decidualizing uterine endometrium and myometrial smooth muscle; later, PAM expression is apparent in the cardiogenic region [64]. PAM expression in the central nervous system exhibits a complex developmental pattern. Nonneuronal cell populations that express especially high levels of PAM include limb mesoderm and the mesenchyme adjacent to nasal, maxillary, palatal and dental epithelia during tissue fusion and remodeling [64]. It is not yet clear whether expression of PAM indicates that amidated peptides or perhaps fatty acyl amides are playing a developmental role in these tissues [65].

Expression of PAM is detectable in many neuroendocrine tumors, and amidated peptides may contribute to tumor growth [60, 66, 67]. For example, small cell lung carcinoma cells secreting gastrin-releasing peptide exhibit decreased growth in the presence of a neutralizing antibody [67]. The growth-promoting role of many amidated peptides makes PAM a target for therapeutic strategies [65].

At least in some cases, α-amidation is the rate-limiting step in peptide production. Thus, raising or lowering the level of PAM protein by transfection with sense or antisense PAM vectors results in a corresponding increase or decrease in peptide α-amidation [12]. The growth of lung tumor cell lines is slowed upon antisense-mediated decreases in PAM expression [68]. Consistent with a rate-limiting role for amidation, levels of PAM synthesis in melanotropes are 10,000-fold lower that levels of substrate (proopiomelanocortin) synthesis, and it is estimated that each secretory granule contains an average of one molecule of PAM [69].

As might be expected for a rate-limiting enzyme, levels of PAM messenger RNA (mRNA) and activity are regulated in a tissue-specific manner, often in parallel with the propeptide substrate [69, 70; reviewed in 12, 23]. For example, castration increases the ratio of glycine-extended substance P to amidated substance P up to sevenfold in specific brain regions [33]. Levels of PAM mRNA in the pituitaries of female rats vary through the estrus cycle and are inversely related to estradiol levels (fig. 3) [71]; in ovariectomized rats, estradiol reduces levels of PAM by an effect on mRNA half-life [72].

Pharmacological inhibitors of PHM and PAL

Disulfiram, used daily by an estimated 200,000 Americans as an alcohol deterrent, reduces levels of amidated peptides in the pituitary and cerebral cortex of adult rats, presumably by chelating copper and inhibiting PHM [33, 73]. Following disulfiram treatment, PAM protein extracted from rat pituitary or atrium and assayed in the presence of optimal levels of exogenous

copper exhibits an unexplained increase in activity [73]. Similarly, the PHM catalytic core prepared by limited trypsin digestion from disulfiram treated rats continues to exhibit an increased V_{max} [74].

Trans-styrylacetic acid (phenylbutenoic acid) is a mechanism-based inhibitor of PHM [53, 75]. When used in vivo, *trans*-styrylacetic acid decreased serum PHM activity 76 and decreased the inflammatory response observed in response to carrageenan [61]. Results of experiments using *trans*-styrylacetic acid and *trans*-styrylthioacetic acid to inhibit PHM from rat, horse and human serum suggest that there are species-specific differences in the response [77]. Other inhibitors of PHM include benzylhydrazine [78] and *N*-acetylphenylalanyl acrylate [79]. N-substituted dipeptides with a C-terminal homocysteine are also potent inhibitors of PHM and effectively block production of amidated substance P in cultured dorsal root ganglion neurons [80, 81]. Potent inhibitors of PAL include pyruvate-extended N-acetyl amino acids [82] and 2,4-dioxo-5-acetamido-6-phenylhexanoate [79].

Requirements for peptide amidation: copper and ascorbate

To date, it appears that all peptide α-amidation is catalyzed by PAM. Immunohistochemical localization of PHM in the absence of PAL has led to the suggestion that additional enzymes are involved, but none has been identified [83]. The amidation of newly synthesized peptides occurs within the lumen of the secretory pathway and requires molecular oxygen, reduced ascorbate and copper along with the peptidylglycine substrate (fig. 4). It has been demonstrated, both in vivo and in vitro, that copper chelators or ascorbic acid deprivation results in a decrease in peptide α-amidation [23, 73, 84, 85].

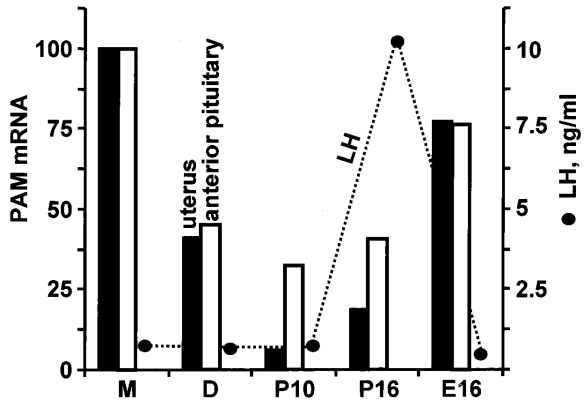

Figure 3. Expression of PAM is Regulated. Levels of PAM mRNA in the anterior pituitary and in the uterus of female Sprague-Dawley rats are inversely proportional to circulating levels of estradiol. This dependence is observed during the estrus cycle of normally cycling female rats. Levels of PAM mRNA were normalized to levels of a control mRNA (S26), with the level at metestrus set to 100%. Levels of plasma luteinizing hormone (LH) verified the stage in the estrus cycle; levels of estradiol also peak at P16. M, metestrus; D, diestrus; P10, proestrus, 10 h; P16, proestrus, 16 h; E16, day of estrus, 16 h. Redrawn from [71] and [72].

A family of sodium-dependent ascorbate transporters responsible for the high-affinity uptake of ascorbate from plasma into cells was recently identified; SVCT2 is especially enriched in neurons, neuroendocrine cells, exocrine cells, osteoblasts and endothelial cells [86]. How cytosolic ascorbate then enters the lumen of the secretory pathway is not clear, although the aqueous pore through which proteins enter the endoplasmic reticulum [87, 88] could provide a pathway. Ascorbate, present at a level of 2–5 mM in the cytoplasm of peptide-producing cells [89–91], may be concentrated 10-fold during the creation of mature secretory granules. Maintenance of reduced ascorbate within the secretory pathway involves shuttling of electrons by cytochrome b_{561} [92] (fig. 4). Other single-electron reductants can substitute for ascorbate in intact cells and in test-tube assays [16, 19–21]. The lack of reductant specificity in PHM is supported by the observation that no ascorbate binding site was identified in crystals of PHM analyzed in the presence of high levels of ascorbate [93].

As discussed in detail below, copper plays an essential role in peptide amidation; no other metal ion can replace copper. The unique chemical properties of copper that give it an essential role in peptide amidation and other processes such as cellular respiration, free-radical defense, connective tissue biosynthesis and cellular iron metabolism mean that copper must be compartmentalized and tightly regulated [94]. Recent studies on two disorders of copper metabolism, Menkes syndrome and Wilson disease, have identified homologous P-type adenosine triphosphatases (ATPases) responsible for transport of copper into the lumen of the secretory pathway (fig. 4) [94–98]. Based on their sites of expression, Menkes protein (MNK) is likely to transport copper into the lumen of the secretory pathway where it could become available to PHM. Increased stimulation of plasma PAM activity by added copper is reported in Menkes patients [99]. Copper binds tightly to many proteins, raising the possibility that a specific copper chaperone may be required to present copper to PHM [100–103]. It is not yet clear when during its biosynthesis PHM acquires the copper atoms that are essential to its function. A soluble PAM protein retained in the endoplasmic reticulum by appending a KDEL-retention/retrieval motif is fully active when assayed with exogenous substrate and copper [104].

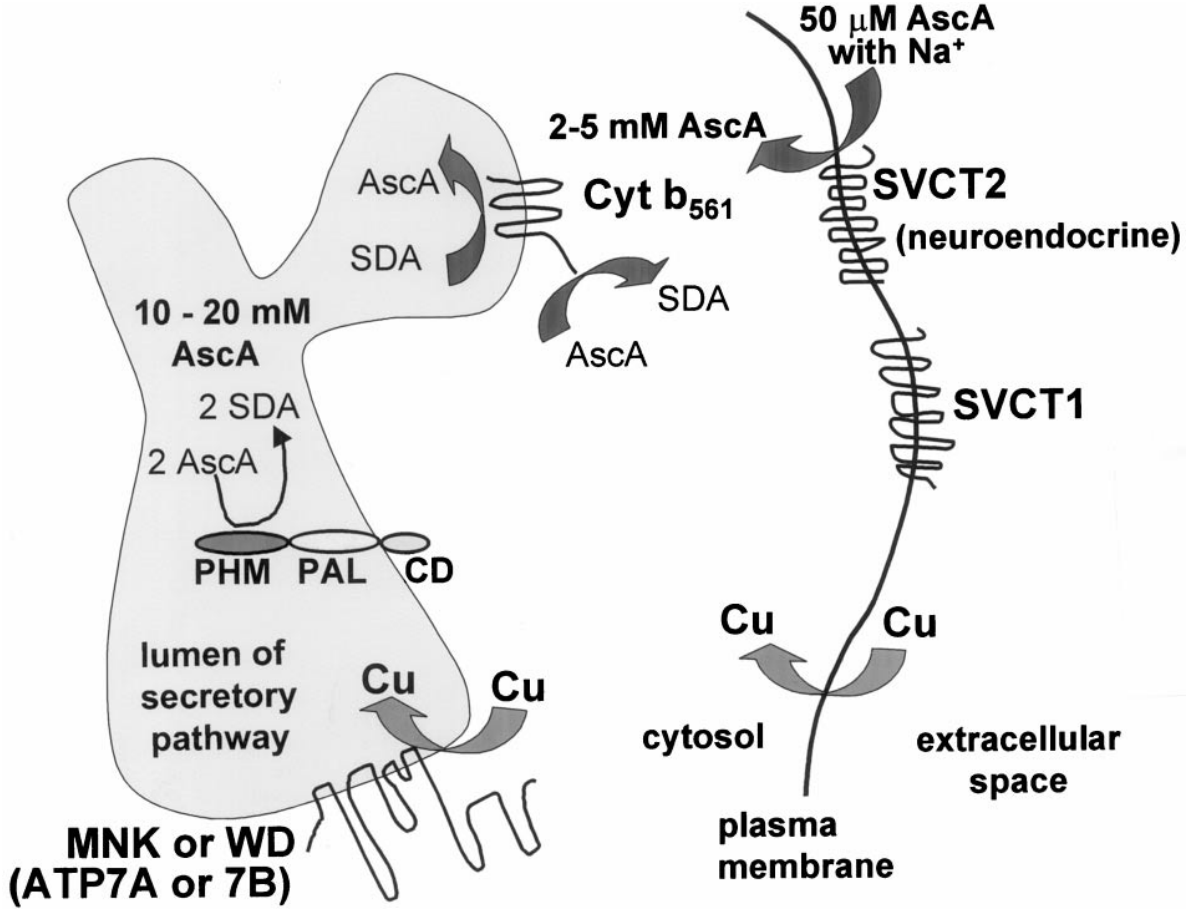

Figure 4. PAM Requires Copper and Ascorbate in the Lumen of the Secretory Pathway. Ascorbate is transported into cells by Na^+-dependent ascorbate transporters (SVCTs); SVCT1 is prevalent in epithelial cells, whereas SVCT2 is prevalent in pituitary and brain [86]. Cytosolic ascorbate levels are 2–5 mM in pituitary and brain, whereas levels of ascorbate in secretory granules are 10–20 mM [91]. PAM converts lumenal ascorbate into semidehydroascorbate, which is reduced to ascorbate in a cytochrome b_{561}-mediated process that depends on cytosolic ascorbate [92, 166]. Cytosolic copper can be transported into the lumen of the secretory pathway by either of two P-type ATPases: the protein that is mutated in Menkes syndrome (MNK; ATP7A) is widely expressed, whereas the protein that is mutated in Wilson disease (WD; ATP7B) is most prevalent in liver.

No consensus has been reached on the mechanisms involved in routing soluble proteins into secretory granules [105–109], but soluble, monofunctional PHM and PAL are each efficiently targeted to secretory granules [110]. In contrast, integral membrane forms of PAM are largely localized to the *trans*-Golgi network region of AtT-20 cells [111]. PAM is one of the few integral membrane proteins associated with peptide-containing secretory granules, and has been used as a tool to investigate the routing of membrane proteins to peptide-containing granules [110–112].

The ability to produce amidated peptides is not limited to classical peptide-producing cells. Even the levels of PAM in fibroblast lines such as NIH-3T3, COS-7 and CHO allow amidation of secretory products engineered to have a C-terminal Gly [113, 114]. Expression of glycine-extended salmon calcitonin in the rabbit mammary gland yields milk containing large amounts of amidated calcitonin [115].

The PAM gene

Detailed studies of the single-copy PAM gene in the rat indicate that tissue-specific alternative splicing generates mRNAs encoding more than seven different PAM proteins [23, 116–118]. The major splicing events result in deletion of exon A (exon 16) and/or deletion of the transmembrane domain (exon 25). Deletion of exon A limits the ability of endoproteases to separate the PHM

and PAL enzymes. Deletion of the transmembrane domain converts membrane PAM into a soluble, lumenal protein that is secreted along with its peptide products. Similarly, alternative splicing of the single-copy human PAM gene generates a collection of PAM proteins [119, 120].

Soluble PHM and PAL proteins are generated from membrane precursors by tissue-specific endoproteolytic cleavage [12]. The activity of the monooxygenase is increased upon removal of the C-terminal region of PAM [121]. As for many multifunctional enzymes, protease treatment demonstrated that PAM is composed of protease-resistant PHM and PAL enzymes [122]. The PHM catalytic core (PHMcc) was refined to rat PAM-1(42–356) by truncation analysis [123]. Similarly, the PAL catalytic core (PALcc) was refined to rat PAM-1(498–820) [124].

Different species have taken different approaches to accomplishing the task of peptide amidation (fig. 5). In the vertebrates, a bifunctional enzyme like that characterized in the rat plays a major role. The rat PAM gene consists of at least 27 exons and encompasses over 160 kb of genomic DNA [118]. This gene is unusual in the large size of many of its introns (4 of the introns are over 10 kb long). Two PAM genes have been identified in *Xenopus laevis*, a species that is thought to be tetraploid [125]; both genes encode bifunctional PAM proteins lacking an exon A-like region. As in the rat, alternative splicing of the *Xenopus* PAM gene can yield monofunctional PHM.

A search of the *C. elegans* database for genes that could encode proteins homologous to rat PAM identifies one bifunctional PAM protein and a separate monofunctional PAL protein (fig. 5); the corresponding cDNAs

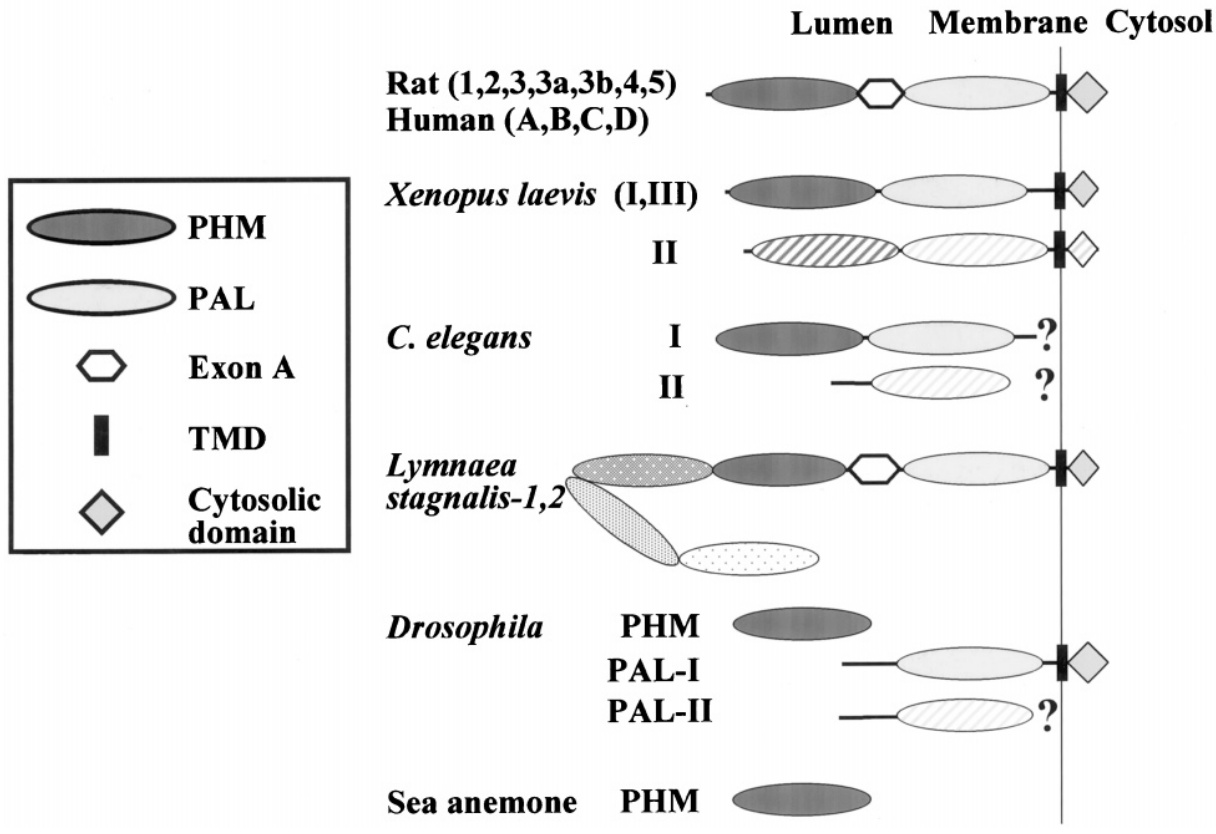

Figure 5. Evolution and the Bifunctional PAM Gene. The proteins encoded by the PAM genes identified in the various species are drawn to scale. Separate genes identified in the same species are listed on separate lines; alternatively spliced variants of the same gene are listed in parenthesis. Not all of these proteins have been expressed and shown to be active. The ? indicates that it is not clear whether a transmembrane domain and cytosolic domain are present. Rat PAM [118]; human PAM [119, 120]; *Xenopus laevis* PAM [125]; *C. elegans*: bifunctional PAM, AAB37637.1 or AAC16983.1; monofunctional PAL, AAB42278.1; *Lymnaea stagnalis* PAM [126]; *Drosophila melanogaster* PHM [11]; sea anemone PHM [127].

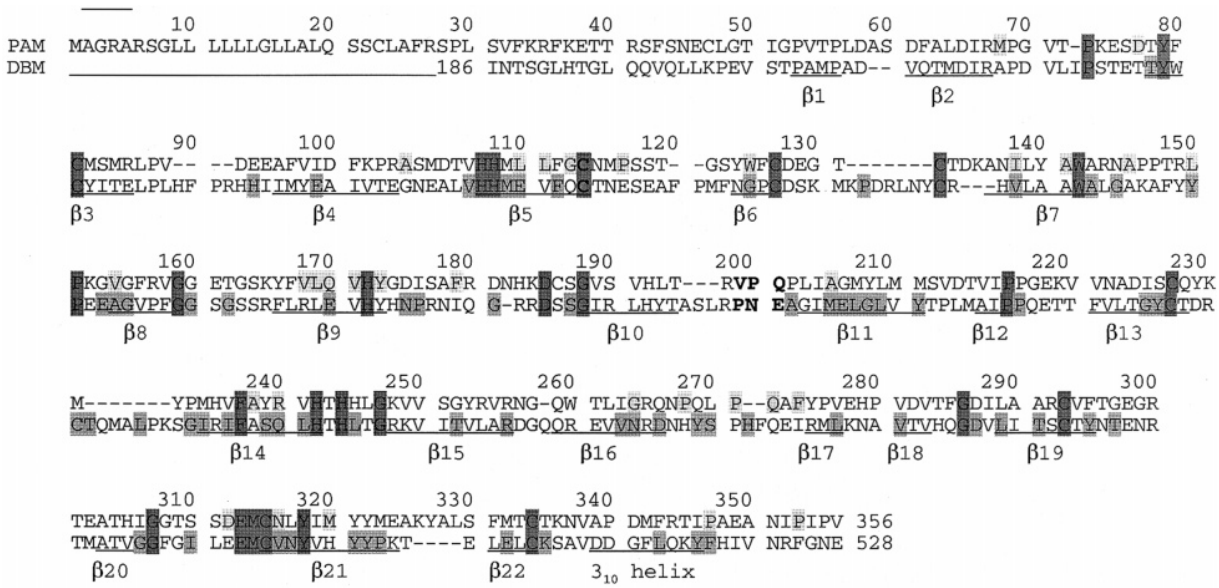

Figure 6. The PHM/DBM Family of Proteins. Twelve PHM sequences (mouse, human, bovine, *Xenopus* I, *Xenopus* II, *Lymnaea* 1–4, sea anemone, *C. elegans* and *Drosophila*) were aligned to the sequence of rat PHM; residues that are identical in PHM of all species are highlighted in light gray or dark gray; although *C. elegans* PAM lacks residues corresponding to Cys81 and Cys126, these residues are still shown as conserved. The locations of each β-strand and the 3_{10} helix are shown. The sequence of rat DBM was aligned to the sequence of rat PAM. DBM sequences from mouse, bovine, horse, human, *Drosophila* and *C. elegans* were aligned to rat DBM, and residues identical in DBM of all species are highlighted in medium gray or dark gray. Identities common to PHM and DBM are highlighted in dark gray.

have not been expressed and shown to encode active enzyme. In *Lymnaea stagnalis*, the pond snail, a single integral membrane protein contains four independent, functional PHM enzymes and a single, active PAL enzyme [126] (fig. 5). Interestingly, alternative splicing of the noncatalytic exon A region also occurs in a cell-type specific fashion in *Lymnaea*.

In contrast, in *Drosophila melanogaster* and in sea anemone, no bifunctional PAM protein has been identified, and separate genes encode PHM and PAL [11, 127]. The exon/intron structure of *Drosophila* PHM is closely related to that of rat PAM. Multifunctional enzymes frequently occur as separate monofunctional enzymes in more primitive species [128–130]. In species in which formerly independent catalytic units are joined together, functional units are often separated by highly variant regions of sequence. Consistent with this, the protease-sensitive region between PHM and PAL, corresponding to exon 15 in rat PAM (fig. 1), is highly species-specific [118]. The monofunctional PHM found in *Drosophila* terminates in the exon that corresponds to exon 14 of rat PAM. A search of the *Drosophila* genome identified two potential monofunctional PAL proteins (fig. 5). A search with TBLASTN of the *Saccharomyces cerevisiaea* genome using the sequence of rat PAM fails to reveal homologs of PHM or PAL.

Residues absolutely conserved in 13 known PHM proteins are identified in figure 6. Only 60 of the 315 residues in the catalytic core are completely conserved when species as diverse as the sea anemone and *Drosophila* are included in the comparison; it is important to note that not all of the PHM proteins included in the sequence comparison have been shown to be active. Nevertheless, the five His residues and the single Met residue which interact with the two essential copper ions are conserved, as are eight cysteine residues, which form structurally crucial disulfide bonds. Many of the other conserved residues are Gly and Pro residues.

The PHM/DBM family of monooxygenases

The only enzyme exhibiting homology to any part of PAM is dopamine β-monooxygenase (E.C.1.14.17.1), a two-copper monooxygenase which catalyzes the ascorbate and molecular-oxygen-dependent conversion of dopamine into norepinephrine [131]. The catalytic core of PHM is 28% identical to the corresponding region of DBM (fig. 6). Eight of the 10 Cys residues in PHMcc are conserved in DBM, and disulfide bonds occur in

homologous locations [123, 132]. The conserved exon/intron junctions in the PHM and DBM genes confirm their evolutionary relationship [118, 133]. The cDNA for a third PAM homolog, monooxygenase X or MOX, was recently discovered by screening senescent human fibroblasts; it is not clear whether MOX is a functional enzyme, and a substrate remains to be identified [134].
Genes encoding PHM and DBM have been identified in multicellular eukaryotes (fig. 6). In *Drosophila*, tyramine β-hydroxylase replaces dopamine β-hydroxylase [135]. A screen of the *C. elegans* genome identifies a DBM-like protein distinct from the PAM and PAL genes shown in figure 5. *Cnidarians*, the most primitive organisms to have an organized nerve net, use amidated peptides but not catecholamines for intercellular communication. Thus, PHM appears to be the evolutionary precursor of DBM [41]. Complete and partial genomes from archaea, eubacteria and single-cell eukaryotes contain no identifiable homologs to either enzyme.

PHMcc crystal structure

Enzymes of the PHM/DBM family are of fundamental importance in many biological processes, and have long been the subject of efforts to better understand the role of copper in bioinorganic chemistry. We used crystals of the nonglycosylated, 35-kDa PHMcc to study the structure and mechanism of this enzyme. Experiments using *N*-α-acetyl-3,5-diiodotyrosylglycine (Ac-DiI-YG), a dipeptide substrate of PHMcc, showed that PHMcc is active in these crystals [93]. Three forms of PHMcc were crystallized and their structures determined by X-ray diffraction methods: (i) oxidized (ox-PHMcc), (ii) reduced (red-PHMcc) and (iii) oxidized with bound substrate (ox-PHMcc/sub) [93, 136]. In all three forms the protein adopts the same overall structure, with only small differences in the conformations of a few active-site side chains and in the coordination geometry of the coppers. The structure consists of two copper binding domains, each about 150 residues in length, comprised primarily of β-strands (fig. 7). The two domains, connected by a three-residue linker, form an oblate ellipsoid with approximate dimensions of 55 Å by 45 Å by 25 Å.

Domain I

The amino-terminal domain (right, fig. 7) is composed of 10 β-strands and binds the copper designated as CuA. The main structural unit is a β-sandwich of two antiparallel β-sheets—one containing four strands, one containing five. Two of the β-sandwich strands, strands 4 and 7, contain classic β-bulges. There are three disulfide links connecting strands and loops in domain I without linking the two β-sheets together.

Domain II

Domain II (left, fig. 7) is composed of 12 β-strands and one 3_{10} helix and binds CuB. The major structural unit is a β-sandwich formed by one four-stranded antiparallel β-sheet and one five-stranded mixed β-sheet. Two of the strands, strands 14 and 16, contain classic β-bulges. There are two disulfide bonds in domain II, both of which connect the two sheets of the β-sandwich.

Overall structure

The two PHM domains differ in many ways, but contain a similar topological core: an eight-stranded antiparallel β-sandwich. When superposed, 86 of their residues overlap with an r.m.s. distance between the α carbons of 1.5 Å. However, when domains I and II are structurally aligned, their sequence identity is less than 5%. Neither the disulfide-forming cysteines nor the copper ligands are conserved. In fact, the CuA and CuB sites are located topologically on opposite sheets of the β-sandwich domains (fig. 8A). Despite the low sequence identity, subtle structural details are conserved between the domains. For example, the β-bulges in domain I (in strands 4 and 7) superimpose exactly on the β-bulges in domain II (in strands 14 and 16).
The orientation of the two domains places the two endogenous coppers, CuA and CuB, 11 Å apart facing the interdomain space. In this region, no part of either

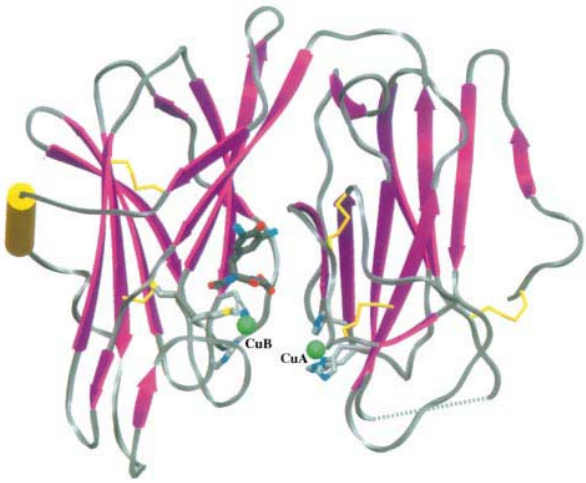

Figure 7. Representation of the PHMcc Fold. The backbone is shown in gray with the coppers represented by green spheres. Strands are purple arrows, and the orange cylinder is a 3_{10} helix. Side-chain ligands to the two catalytic coppers are colored by atom type (carbon is gray, nitrogen is blue and sulfur is yellow). Bound substrate is shown in dark grey. This figure was made with the program SETOR [167].

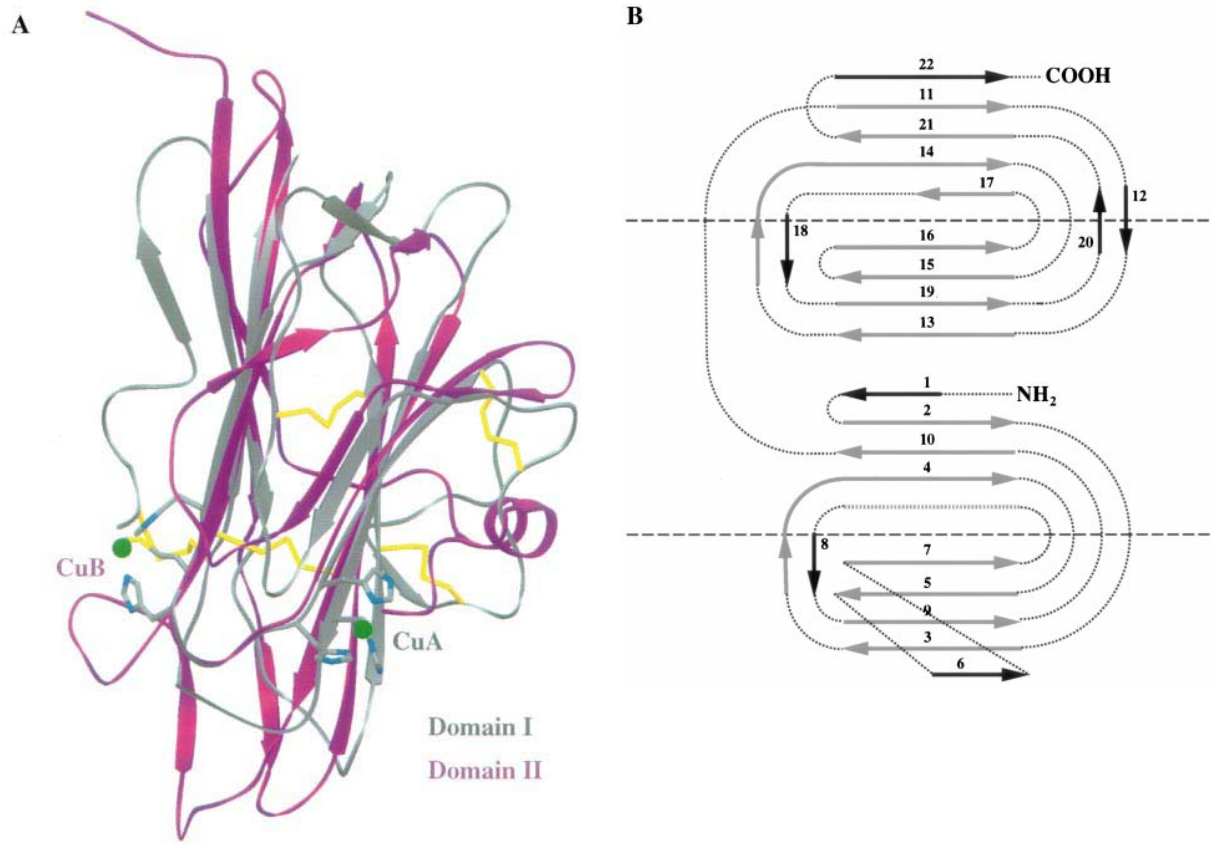

Figure 8. Topology of PHMcc Domains. (*A*) Superposition of domain I and domain II of PHMcc. Domain I (grey) is shown superposed on domain II (purple) based on the structural alignment of 86 residues from each domain (the α-carbons of these residues align to 1.5 Å r.m.s. distance). (*B*) Topology of PHMcc. Both domains of PHMcc are shown with numbered strands represented as solid arrows and the connecting loops represented by dotted lines. The β-sheets in both domains are separated by a dashed horizontal line. The eight-stranded topological core found in both domains of PHMcc is shaded in gray.

domain is in contact with the other, leaving the cleft between the two coppers accessible to solvent. In a region distant from the copper binding sites, the two domains are closely associated through a large hydrophobic interface formed by residues well conserved in PHM sequences (515 Å^2 of domain I and 500 Å^2 of domain II are buried). The interdomain interface is further stabilized by a hydrogen-bonded antiparallel β-sheet that links the two domains.

Comparison with other proteins

The Brookhaven Protein Data Bank contains several proteins whose three-dimensional structures are similar to those of PHMcc. The DALI search engine [137] was used to match protein topologies by preserving the sequence order of secondary structural elements—in this case the order of strands in the β-sheets. The two domains of PHMcc have similar topologies, forming eight-stranded antiparallel jelly-roll β-sandwiches (fig. 8B). Domains with this topology are found in many viral capsid proteins, lectins and glucanases, although no detectable sequence identity exists between PHM and any of these proteins. One domain of the copper-binding enzyme galactose oxidase, has a topologically similar jelly-roll domain, but the enzyme does not use this domain to bind its copper atoms.

The endoglycosidase asparagine amidase (EC 3.5.1.52) is the only protein to match a region spanning both domains of PHMcc in overall structure. Asparagine amidase does not bind metal atoms and catalyzes the deglycosylation of N-linked carbohydrates—a reaction dissimilar to the PHM/DBH reaction. The structural search matched 201 of 311 residues from asparagine amidase with 201 of 315 PHMcc residues. Over the 201 residue region, the sequence identity is 4%, a nonsignifi-

cant identity, yet the peptide backbone positions of the two proteins differ by only 5.0 Å r.m.s. distance. The asparagine amidase structure contains four β-bulges which align near the four β-bulges found in PHMcc. Three of the β-bulges are shifted by one residue relative to PHMcc, whereas the fourth is shifted by three residues. The structural similarity between the two proteins suggests an evolutionary relation.

PHM spectroscopic studies

Extensive spectroscopic data have been reported for the coppers of PHM and DBM. These studies showed that the two coppers, named CuA and CuB, are far apart and do not form a dicopper center. Extended X-ray absorption fine structure (EXAFS) experiments indicate an average of 2.5 N (histidines) and 1.5 N or O ligands per copper atom in the oxidized state [13, 138, 139]. One study indicated the presence of a weak sulfur ligand to CuB in oxidized PHM [13]. In the reduced state, EXAFS readily detects a sulfur ligand to CuB in both enzymes [138–140]. Fourier transform infrared (FTIR) spectroscopy on anaerobic, reduced PHM in the presence of CO (an O_2 analog) showed that CO binds to reduced CuB, presumably forming a four-coordinate complex [139]. A similar study in DBM showed that CO binds to CuB competitively versus oxygen [141, 142]. These studies identify CuB as the copper associated with oxygen binding and the chemical steps of the reaction. Our determination of the high-resolution structure of PHMcc provided the first complete description of the copper sites [136].

Copper coordination

The general characteristics of the copper coordination are similar in all three structures of PHMcc; the small differences in coordination of the coppers in the three forms will be described in later sections.

Domain I binds one active site copper (CuA) with three histidine Nδ ligands (H107, H108 and H172). The coordination geometry of CuA is T-shaped, with H107 and H108 at the top of the T and H172 at the base (fig. 9A,B). The Cu–Nδ bond lengths are short for H107 and H108 (1.9–2.2 Å) and longer for H172 (2.1–2.6 Å). Domain II binds the second catalytic copper (CuB) with two histidine Nε ligands and a methionine sulfur (H242, H244 and M314). A solvent ligand (probably water) also binds to CuB, forming a tetrahedral complex (fig. 9A,B). The Cu–Nε bond lengths for H242 and H244 are about 2.0–2.2 Å, whereas the Cu–Sδ M314 bond is considerably longer (2.4–2.6 Å). All six copper ligands are conserved among PHM sequences (fig. 6), and mutagenesis of any of these residues eliminates PHM activity [13, 123, 143].

Structures of different PHMcc states

The structures of oxidized, reduced and substrate-bound oxidized PHMcc show small but significant differences that provide insight into how key events in the PHM reaction cycle may occur.

Oxidized and substrate-bound oxidized PHMcc

In the presence of oxygen, oxidized PHMcc is the

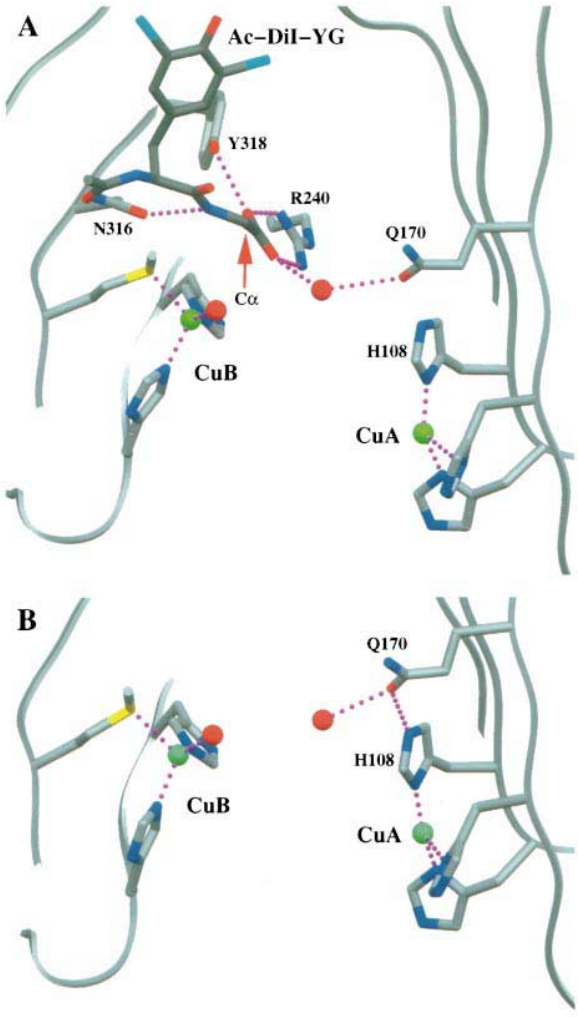

Figure 9. Reduced and Oxidized PHMcc Active Sites. (*A*) Oxidized PHMcc active site (ox-PHMcc/sub). Peptide substrate is shown colored by atom type (carbon is gray, nitrogen is blue, oxygen is red, sulfur is yellow and iodine is turquoise). The copper atoms and waters are represented by green and red spheres, respectively. Dotted purple lines indicate hydrogen bonds or copper ligation. In the oxidized state, a water bridges the peptide substrate and Q170, but Q170 does not form a hydrogen bond with H108. A red arrow indicates the reactive α-carbon of the substrate glycine. (*B*) Reduced PHMcc active site (red-PHMcc). The backbone is shown in gray with important active-site residues colored by atom type. This figure was made with the program SETOR [167].

resting form of the enzyme. The initial structure determination was done with this form. Subsequently, cocrystals were grown of a PHMcc/substrate complex (ox-PHMcc/sub). The substrate *N*-α-acetyl-3,5-diiodotyrosylglycine (Ac-DiI-YG), was used since this compound is a substrate for crystalline PHMcc [93] as well as PHMcc in solution ($K_m = 3$ μM). Crystallization was carried out by adding excess Ac-DiI-YG to the crystallization conditions. This approach ensures that the crystals are oxidized, since any reduced PHMcc would rapidly react with the substrate, producing oxidized PHMcc in the process. The structure should include any structural changes induced by substrate binding since the substrate binds to PHMcc before the complex crystallizes.

Comparison of the structures of oxidized PHMcc with and without bound peptide reveals no significant differences, either in the conformations of individual residues or in overall structure (0.3 Å r.m.s. for α-carbons). The CuA–CuB distance is about 11 Å in both structures: binding of peptide does not bring the two domains into closer proximity. The most significant structural change upon peptide binding is a rotation of the N316 side chain (30° rotation of χ-2), breaking a hydrogen bond with Y318 and forming a new hydrogen bond with the backbone of the substrate.

The ox-PHMcc/sub structure reveals that the substrate binding site is exquisitely tailored to bind peptidylglycine (fig. 9A) without relying on specific side-chain interactions. Several conserved active-site residues (R240, Y318 and N316) and one structural water form hydrogen bonds with the peptide backbone of the bound substrate, anchoring it in the interdomain cleft (figs 7 and 9A). The Ac-DiI-YG carboxylate is anchored by a bidentate salt bridge to the guanidinium of R240 and a hydrogen bond to Y318, and the glycyl NH makes a hydrogen bond with the side chain of N316. The diiodotyrosine side chain occupies a loose hydrophobic pocket which is spacious enough to accommodate any amino acid side chain. In addition, several hydrophobic residues have extensive contact with the substrate, including CuB ligand M314 [139]. The reactive Cα of the substrate glycine is 4.4 Å from CuB, and the *pro-S* hydrogen (abstracted during the PHM reaction; [144]) is oriented towards the CuB-bound solvent atom.

Mutational studies confirm the importance of key active site residues. For example, replacement of Y318 with phenylalanine increased the K_m of PHMcc for peptidylglycine substrate about seven-fold with little effect on V_{max} [123]; replacement of M314 with isoleucine resulted in an inactive enzyme that bound less tightly to peptidylglycine resin than wild-type PHMcc [13].

Reduced PHMcc

Reduced PHMcc crystals (red-PHMcc) were made by soaking crystals in 5 mM ascorbic acid, a concentration that reduced the copper sites in identical crystals during crystal activity experiments [93]. Once reduced, the coppers remained reduced, since oxidation of the copper atoms requires both substrate and oxygen [15]. Red-PHMcc and ox-PHMcc/sub represent different ligand states and oxidation states, yet are structurally very similar. The r.m.s. distance (α-carbons) between red-PHMcc and ox-PHMcc/sub is 0.3 Å. The two CuA–CuB distances are not significantly different: 10.4 Å in red-PHMcc, 10.6 Å in ox-PHMcc/sub. Taken together, these results indicate that neither reduction nor substrate binding results in significant interdomain motion.

The red-PHMcc structure (fig. 9B) supports a model in which ascorbate reduces CuA and CuB independently. Ascorbate (5 mM in the mother liquor) is not found near either copper in red-PHMcc, indicating the absence of a tight ascorbate binding site. This conclusion is supported by the observation that several one-electron donors can be used instead of ascorbate [16, 19–21]. It is likely that reductants interact directly with each copper, relying on the exposure of both coppers to solvent. This mechanism of reduction is attractive because it allows independent reductions of the two coppers without requiring electron transfer between the metals in the absence of bound substrate. Both coppers of PHM are known to be reduced by ascorbate in the absence of substrate [15].

The most noticeable differences between the PHMcc structures involve changes in the positions of Q170 and H108 (fig. 9A,B). In red-PHMcc, H108 and Q170 form a hydrogen bond (Fig. 9B); in ox-PHMcc, a water molecule bridges H108 and Q170 (data not shown). Different interactions occur in ox-PHMcc/sub—a water molecule occupies a position between the side chain of Q170 and the carboxylate oxygen of the bound substrate (fig. 9A). An ox-PHMcc/sub $2F_o - F_c$ map (calculated before water molecules were placed) contoured at 1σ shows electron density connecting the side chain of Q170 to the substrate carboxylate (the distance from the Oε of Q170 to the carboxylate oxygen of Ac-DiI-YG is 5.6 Å). A water molecule placed in this density is about 3 Å from Q170 and 3 Å from the substrate carboxylate.

Mechanism of the PHM reaction

Mechanistic insight from the DBM reaction

The PHM and DBM reactions have been studied extensively. Despite marked differences in their substrate specificity, the reaction mechanisms of the two enzymes appear to be highly similar [145]: both exhibit catalytic

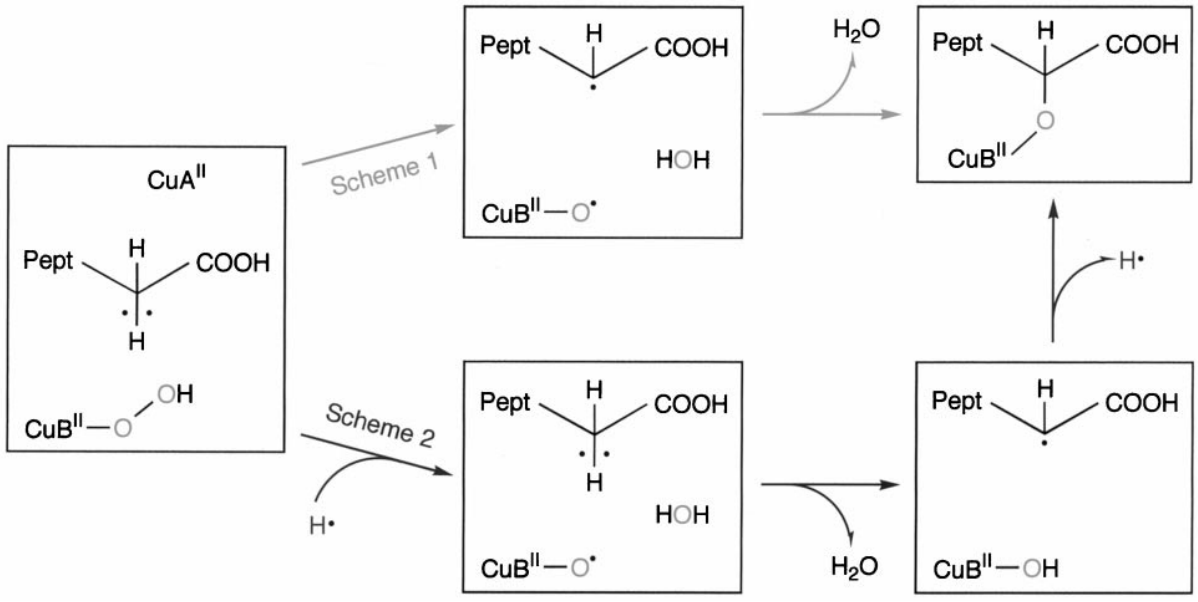

Figure 10. Possible PHM Reaction Schemes. Scheme one (top) and scheme two (bottom) show two possible routes from peptide substrate to alkoxide product based on two mechanistic proposals for DBM [146, 154]. Gray shaded atoms mark atoms mark key atoms during the reaction.

competence of the reduced enzyme, were shown to involve a radical intermediate, have the same stereospecificity of abstraction and involve addition of oxygen from molecular oxygen to an activated aliphatic carbon [146–148]. Data from the two systems have been used to complement each other. In this section we describe the mechanistic proposals as they apply to PHM. The main experimental evidence can be summarized as follows:

1) Starting with oxidized PHM, the resting form of the enzyme, the two coppers are reduced from Cu^{2+} to Cu^{+} by two one-electron transfers from two ascorbates oxidized to semidehydroascorbates, which disproportionate to yield ascorbate and dehydroascorbate; this produces catalytically competent reduced PHM [15].
2) Only in the ternary complex of reduced enzyme with peptidylglycine substrate and molecular oxygen does the reaction progress, producing amidated product, water and oxidized enzyme [15].
3) Studies with mechanism-based inhibitors suggest that the reaction progresses through an alkyl radical intermediate [53, 149].
4) Stereospecificity of hydrogen abstraction (*pro-S*; [144]) and chirality of product (*S*; [150]) have been established.
5) Molecular oxygen, not water oxygen, is incorporated into peptidyl-α-hydroxyglycine product [151–153].

Additional kinetic experiments with purified DBM led to the proposal of two alternative chemical mechanisms that differ mainly in the nature of the hydrogen-abstracting species [146, 154]. These mechanisms can be used as starting models for the reaction catalyzed by PHM. In both schemes, molecular oxygen binds to CuB after ascorbate reduces the catalytic coppers. In the presence of substrate, each copper donates one electron to molecular oxygen, which undergoes a two-electron reduction to peroxide. Either solvent or an active site general acid protonates the peroxide, forming copper-bound hydroperoxide [155]. From this point, the two reaction schemes diverge.
In scheme 1 (Fig. 10, top), homolysis of the hydroperoxide is coupled to abstraction of hydrogen from the substrate [146]. Scheme 2 (Fig. 10, bottom) relies on an active-site residue (thought to be a conserved tyrosine) to donate a hydrogen atom (proton and electron) to form a copper-bound radical [154]. Both mechanisms result in a copper-alkoxide complex which dissociates to yield free enzyme and product.

Reaction steps

The crystal structures of PHMcc shed light on how the two reaction schemes shown in figure 10 might operate. Both reaction schemes begin with oxygen binding to one of the active site coppers. The PHMcc structures

show that CuB is solvent-exposed and has a solvent ligand that could be displaced by molecular oxygen binding. This conclusion agrees with EXAFS data which show that CO (an oxygen analog) binds to a copper which is coordinated by a sulfur ligand [139]. Both reaction schemes call for protonation of the copper-bound molecular oxygen [155] either by solvent or a protein general acid. In the PHMcc structure, no general acids are found in the region surrounding CuB. The hydroxyl of Y318 (conserved in all sequences) is 6.8 Å from CuB, and is the closest reactive protein side chain. Thus, solvent would be the most likely proton donor in these reaction schemes.

The second scheme calls for hydrogen transfer from the enzyme to the Cu^{II}-hydroperoxide species, resulting in radical formation on the amino acid donor. Three amino acids have been shown to stabilize radicals in other systems: tyrosine (ribonucleotide reductase, photosystem II, prostaglandin H synthetase, amine oxidase and galactose oxidase), tryptophan (cytochrome c peroxidase and methylamine dehydrogenase) and glycine (pyruvate formate lyase and ribonucleotide reductase) [156]. Two tyrosines (Y79 and Y318) are in the vicinity of CuB, and are conserved in all sequences of PHM and DBM. However, the distance from CuB to the hydroxyls of Y79 and Y318 are 7.67 Å and 6.78 Å, respectively. These distances are too long for direct interaction between tyrosine and copper-bound molecular oxygen. In addition, mutagenesis experiments show that replacement of Y79 and Y318 with phenylalanine does not abolish PHM activity, indicating that these residues are not involved in a critical catalytic step [13, 123]. The Y318F mutant does show a sevenfold increase in K_m, but this increase is probably due to its role in binding peptide substrates in the PHMcc active site.

PHM mechanistic studies

Our structural and mutagenesis studies provided important insight into the mechanism of the PHM reaction. First, they rule out the involvement in catalysis by PHM of the tyrosines proposed as part of scheme 2. Second, by providing the detailed geometry of the groups involved in the reaction, they strongly suggest that the hydrogen abstraction is carried out by a copper-bound oxygen species. These and other observations allowed us to propose a novel mechanism (fig. 11) that, although different from previous proposals, incorporates some of the features of both schemes [93].

One important question that had not been addressed before our structural studies was the pathway used to transfer one electron from CuA to the oxygen bound to CuB as part of the two-electron reduction of molecular oxygen. Our structures show that the two coppers are 11 Å apart [136], and our crystal activity experiments show that this distance does not change significantly during the catalytic cycle [93]. Thus, the enzyme has contradictory requirements: it has to facilitate transfer of an electron from CuA to CuB, but has to prevent liberation of harmful reduced oxygen species that result from the electron transfer. Our structures of PHM suggest a substrate-mediated electron transfer pathway (see below). This allows reduction of molecular oxygen to occur only when substrate is bound to the enzyme. Under these conditions the reduced oxygen species are not released, but instead react immediately with the bound substrate.

Electron transfer

PHM and DBM reaction schemes call for electron transfer from CuA to CuB during the reaction cycle. In other enzymes where electron transfer occurs from more than one metal to one oxygen molecule, the oxygen is bound bridging both metals, or the metals are located close enough for metal to metal electron transfer. In the case of PHMcc, the coppers are separated by an 11 Å solvent-filled cleft between domain I and domain II. Interdomain motion could reduce the distance between the coppers during catalysis, but the available evidence suggests that this mechanism of electron transfer is not operational in PHM. The CuA and CuB ligands are fixed in place by the β-sheets; thus, the movement would have to involve a global hinge motion between the two PHMcc domains instead of local flexibility in the vicinity of the copper binding sites. Hingelike movement of the two PHMcc domains would involve considerable rearrangement of residues in the interdomain interface. Finally, the crystal activity experiments described above show that electron transfer occurs in the crystal phase, where interdomain motion is not possible. In all PHMcc structures, the shortest through-bond electron transfer pathway connecting CuA to CuB is 70 residues in length (about 250 Å), and the shortest pathway including hydrogen-bonded residues is also prohibitively long (24 residues; about 80 Å). These distances are considerably longer than known through-bond electron-transfer distances in proteins, which rarely exceed 40 Å. The rate of electron transfer would be enhanced, however, by the presence of a shorter pathway between the CuA and CuB sites.

The crystal structures of red-PHMcc and ox-PHMcc/sub illuminate a possible mechanism for electron transfer (fig. 9A,B). In the reduced state (red-PHMcc), a hydrogen bond is formed between H108 and Q170 (fig. 9B). In the substrate-bound oxidized state, a water molecule is located between Q170 and the substrate carboxylate (fig. 9A). From these two structures it can be inferred that in the substrate-bound reduced state, the H108–Q170 hydrogen bond exists while a water

molecule is hydrogen-bonded to Q170 and the substrate carboxylate. This positioning of atoms forms a connection between CuA and CuB that may function as an electron-transfer pathway, but only when substrate is bound to reduced PHM. The substrate-mediated electron transfer pathway is about 20 Å in length—well within the range of distances for well-characterized electron-transfer reactions. Calculations with the program PATHWAY [157] support the important role of the substrate in the electron-transfer pathway. The electron-transfer rate calculated [158] for the substrate-mediated pathway (fig. 12A) is 10^7 times faster than the rate calculated with the substrate removed (fig. 12B). This proposal is further supported by experimental data that show that electron transfer does not occur unless substrate is present (i.e. reduced PHM is not reoxidized to Cu^{2+} in the presence of oxygen alone; [15]).

The proposed electron-transfer pathway includes the carboxyl portion of the substrate: the glycyl α-carbon and carboxylate. The same atoms, present in all known peptide substrates, could bind to PHM in a manner identical to the substrate binding observed in ox-PHMcc/sub. PHM substrates and mechanism-based inhibitors include several nonpeptide compounds which contain only these atoms in common [14, 53–56, 77, 149, 159, 160]. Compounds that contain an amide in place of the required carboxylate are not PHM substrates, perhaps due to disruption of the electron transfer pathway. One interesting outcome is that hormones that end in glycylamide (e.g. oxytocin and vasopressin) are generated by PHM from precursors which end in two glycine residues. Once the terminal glycine is cleaved by PAM, the remaining hormone, now terminating in glycylamide, is no longer a PHM substrate.

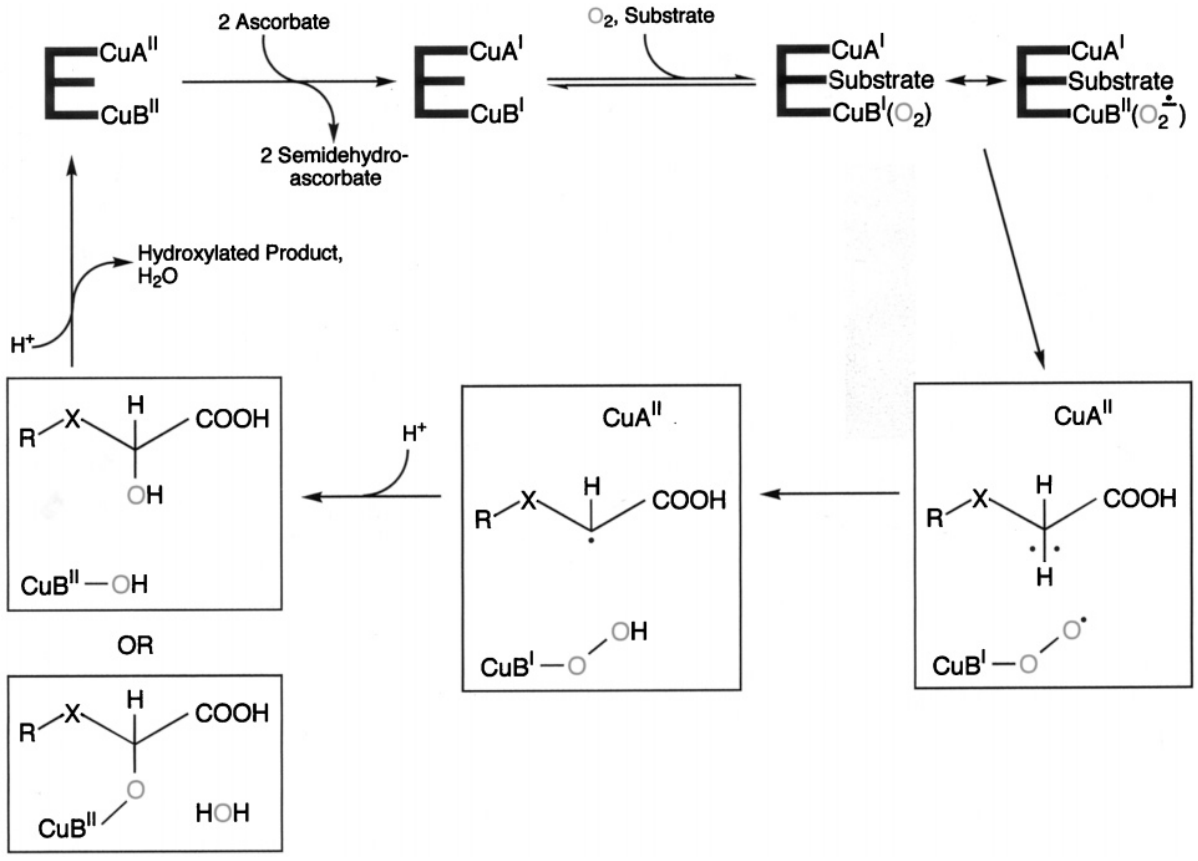

Figure 11. Mechanism Proposed for PHM. Copper-bound oxygen exists in two resonance forms indicated by the double-headed arrow. Oxygen atoms derived from molecular oxygen are shaded gray. The substrate atom labeled 'X' indicates that 'NH', 'O' or 'S' can occupy this position. This mechanism is also compatible with the formation of a copper-alkoxide product (lower left) as proposed for DBM [154, 168].

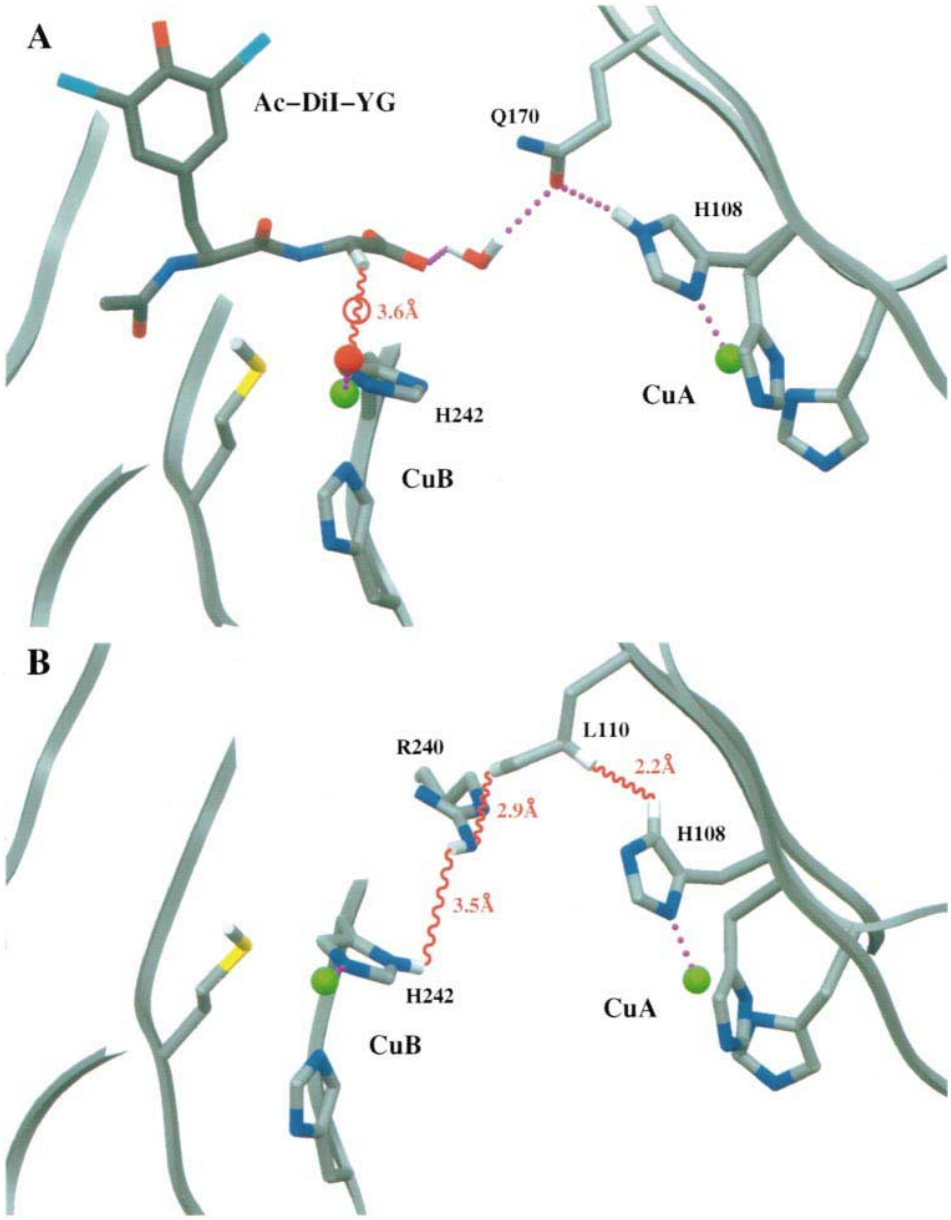

Figure 12. Calculated Electron-transfer Pathways. (*A*) Electron-transfer pathway calculated for ox-PHMcc/sub. The best electron-transfer pathway was calculated with the program PATHWAY [157] and is shown as a combination of through-bond, through-hydrogen bond and through-space jumps. The PHMcc backbone is shown in gray with the coppers represented by green spheres and other atoms colored by atom type. The through-space jump is marked by a wavy red line with the corresponding interatomic jump distance. Copper ligand bonds and hydrogen bonds are indicated with dotted lines. (*B*) Electron-transfer pathway calculated for ox-PHMcc/sub with the substrate and solvent molecules removed. The best electron-transfer pathway from CuA to CuB was calculated with the program PATHWAY [157] and represented as in (*A*). The calculated electron-transfer rate [158] is enhanced by 10^7 in the substrate-mediated pathway (*A*) compared with the pathway shown in (*B*). The open red circle in (*A*) marks a possible position for the second oxygen atom of molecular oxygen based on the geometry of a small molecule Cu-dioxygen structure [169]. The close juxtaposition of dioxygen with the substrate would further enhance the electron transfer rate. This figure was made with the program SETOR [167].

PHM reaction mechanism

Electron transfer through the substrate may be a critical feature of catalysis by PHM, allowing the reaction to proceed only in the presence of substrate and oxygen. In general, a reduced copper dioxygen complex could exist in three resonance states: Cu^{I}-dioxygen, Cu^{II}-superoxide or Cu^{III}-peroxide. The structures of PHMcc show that the CuB site is composed of poor electron-

donating ligands (especially methionine), which would prevent formation of the high-valence cupryl state (Cu^{III}). The Cu^{II}-superoxide resonance form is thought to dominate in small molecule copper-oxygen complexes [161]; however, compounds containing a thioether ligand (similar to methionine) appear to stabilize the Cu^{I} state [162, 163]. Thus, PHM-bound dioxygen may exist in resonance between Cu^{I}B-dioxygen and Cu^{II}B-superoxide (fig. 11) (these resonance states are both electron paramagnetic resonance (EPR)-silent due to spin coupling). Substrate binding provides a pathway for electron transfer from CuA to CuB, with formation of Cu^{II}A (EPR-active) and Cu^{I}B-superoxide. This model provides an explanation for the observation that reduced PHM (EPR-silent) exposed to oxygen remains EPR-silent until substrate is added [15]. The resulting Cu^{I}B-superoxide species could be protonated to yield Cu^{II}B-hydroperoxide. Subsequent steps of the PHM reaction could be similar to the mechanisms described as scheme 1 or scheme 2 in figure 10. Our results, however, suggest a new possibility that does not involve a Cu^{II}B-hydroperoxide species.

In this novel proposal (fig. 11), the distal oxygen of the Cu^{I}B-superoxide abstracts the *pro-S* hydrogen from the α-carbon of the substrate glycine. Small-molecule transition metal complexes indicate that metal-bound superoxide is capable of hydrogen atom abstraction [164]. Structural details in PHM are also consistent with hydrogen abstraction by superoxide; the *pro-S* hydrogen is oriented towards the CuB-bound solvent ligand (see above). The resulting substrate radical attacks the CuB-bound hydroperoxide, promoting homolytic cleavage of the oxygen-oxygen bond. With the addition of a proton (perhaps from solvent), hydroxylated peptide product and a Cu^{II}-hydroxide species are formed. The CuB-bound hydroxyl dissociates with addition of another proton from solvent, regenerating the oxidized enzyme. Alternatively, the last step of the mechanism could involve a copper-bound alkoxide (fig. 11).

The PAL enzyme

Carboxy-terminal and amino-terminal truncations have allowed us to define the catalytic core of PAL (PALcc), and mutagenesis of the N-glycosylation site has shown that PAL activity is not affected by elimination of the sugar side chain [124]. Nonglycosylated PALcc, a 38-kDa protein, appears to be ideal for crystallization trials. Preliminary studies on PALcc indicate that it is extremely resistant to protease digestion. The four cysteine residues in PALcc form two disulfide bonds. The thermal stability of PALcc is decreased following treatment of the enzyme with EDTA [124], suggesting that a divalent metal plays a structural role in this protein. Mutagenesis of potential zinc ligands identifies a set of PALcc proteins that are efficiently secreted but exhibit vastly reduced activity. The structure of PAL will prove interesting from the standpoint of general enzymology since there is no known structural homolog to PAL. In terms of its reaction mechanism, PAL may be closely related to alcohol dehydrogenase, a well-studied zinc-containing enzyme [165]. The structural details of the PAL active site will help to determine whether such a mechanism (fig. 13) is viable.

Other copper monooxygenases: DBM and MOX

Mechanistic insights gleaned from structural studies on PHM may be applicable to all members of the two copper monooxygenase family. Of particular interest are the substrate binding requirements and the position of the catalytically important residues in DBM. To address these issues, rat DBM was modeled using the structure of rat PHM as a template. Rat PHM and rat DBM sequences (27% identical over 314 residues) (fig. 6) were aligned based on the structure of rat PHM. The correct alignment of the six conserved copper ligands anchors most of the active-site residues, increasing confidence in this area of the model. A bound confor-

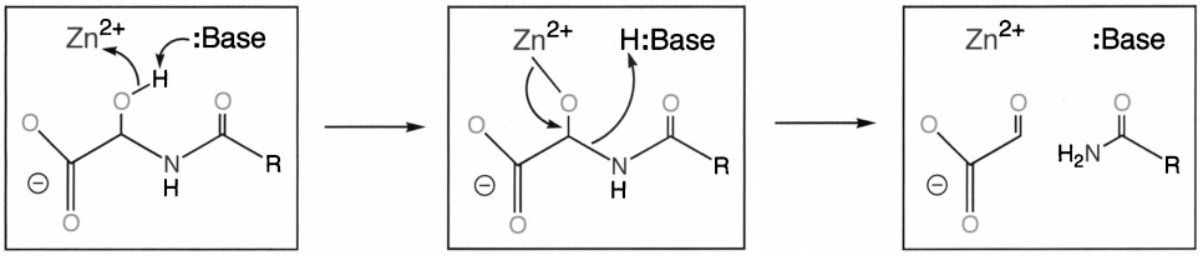

Figure 13. PAL Reaction Mechanism. A hypothetical reaction mechanism for PAL is shown. The mechanism relies on an active site zinc to hydrolyze α-hydroxylated substrate (the product of the PHM reaction).

mation of dopamine was built manually so that the reactive β-carbon occupied the same position as the reactive α-carbon of a peptidylglycine substrate bound to oxidized PHM.

Figure 14 shows the structure of the PHM/peptide complex in the same orientation as the model of the DBM/dopamine complex. In PHM, the substrate glycine is anchored in place by a salt bridge to R240 (fig. 14A). This arginine is conserved in all PHM sequences, but is replaced with glutamine in all DBM sequences (fig. 6) (Q413 in fig. 14B). Dopamine cannot interact directly with Q413 in DBM, but another conserved residue, E268, can form hydrogen bonds with Q413 and dopamine. The salt bridge formed between dopamine and E268 in the DBM model is analogous to the substrate-R240 salt bridge observed in the PHM structure. The dopamine-E268 interaction may be of critical importance in DBM because it forms a connection between the CuA site (nearby H266 is a CuA ligand) and the substrate dopamine which could act as a substrate-mediated electron transfer pathway similar to the one proposed for PHM (see above).

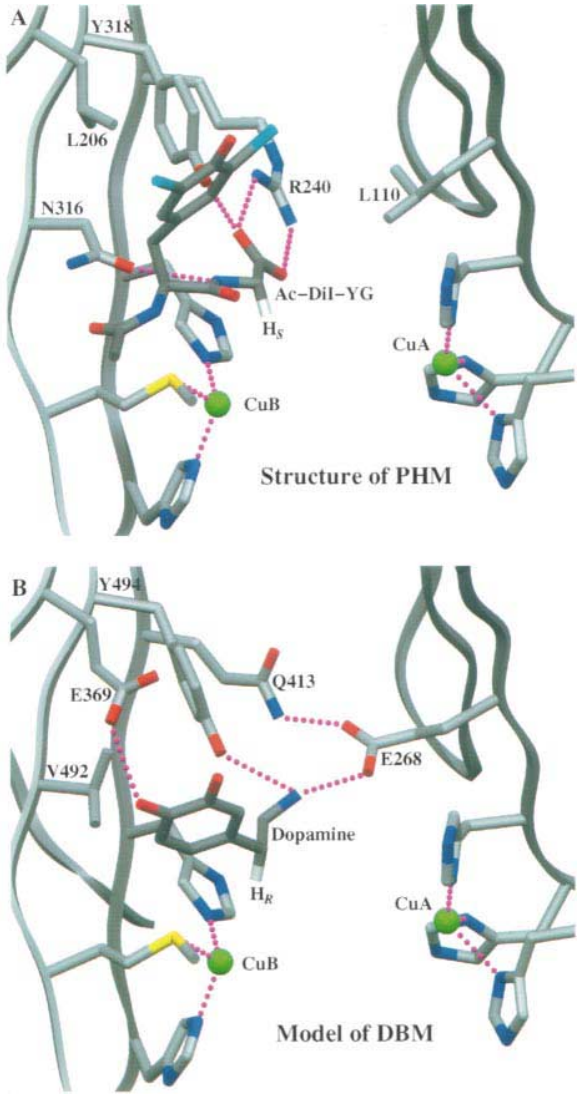

Figure 14. Modeling of the DBM Active Site. (*A*) Structure of the ox-PHMcc/sub active site. The Ac-DiI-YG substrate, copper ligands and five key active-site residues are colored by atom type. Coppers are represented by green spheres, and dotted lines represent hydrogen bonds and copper ligand bonds. (*B*) Model of the DBM active site. The model of DBM with bound dopamine is shown colored as in (*A*). The modeled interactions of dopamine (manually placed) with key active-site residues are shown. This figure was made with the program SETOR [167].

PHM uses N316 to recognize the peptide backbone of its substrates (fig. 14A). In all DBM sequences, a valine (V492 in rat DBM) replaces N316, and may form hydrophobic contacts with the edge of the dopamine ring, orienting the 3′-hydroxyl to face upwards where it will interact favorably with solvent (figure 14B). The active-site tyrosine Y318 (Y494) is conserved in all PHM and DBM sequences. It forms a hydrogen bond with the substrate glycine in PHM and may form a hydrogen bond with dopamine as shown in fig. 14B. In addition, Y494 may help to bind dopamine by forming a hydrogen bond with the π-cloud of the dopamine ring. It is not clear why this tyrosine is so well conserved, since substitution to phenylalanine through site-directed mutagenesis in rat PHM yields an active enzyme with little effect on V_{max} and only a sevenfold increase in the K_m of PHM for peptidylglycine substrate [123].

Rat PHM preferentially binds peptides with a hydrophobic amino acid in the penultimate position (preceding the glycine). In the PHM/substrate structure, L206 interacts with the side chain in the penultimate position (diiodo-tyrosine), and may be a factor in the substrate preference of PHM (figure 14A). In all DBM sequences, a glutamate (E369) replaces L206, and may form a hydrogen bond with the 4′-hydroxyl of dopamine, helping to specifically recognize 4′-hydroxybenzyl compounds such as dopamine and tyramine. Interestingly, L206 is the only residue in fig. 14A that is not conserved in all PHM sequences. *Lymnaea* PAM contains four tandem PHM enzymes that differ in their substrate specificity [126]. The four *Lymnaea* PHM enzymes have leucine, isoleucine and phenylalanine in this position, perhaps to optimize the binding of different substrates. Interestingly, the *Lymnaea* PHM enzyme that has a leucine in this position is most similar to rat PHM in its substrate specificity [126]. Similar modeling of human MOX suggests that MOX is not likely to accommodate either PHM or DBM substrates. In MOX, the positions of the PHM R240 and the DBM E268 are occupied by

leucines, removing the possibility that the residues at these positions may form a salt bridge with the substrate. DBM residues V492 and E369 are similar to the leucine and glutamate found in these positions in MOX, perhaps indicating that the MOX substrate contains a moiety similar to the dopamine ring. The conserved tyrosine seen in PHM (Y318) and DBM (Y494) is also conserved in MOX.

Summary and conclusions

Carboxy-terminal α-amidation is a widespread post-translational modification of peptide hormones, growth factors and neurotransmitters. Activation of peptides that require amidation for full biological activity can be specifically regulated through this process. Two characteristics of the amidation reaction contribute to this additional level of regulatory control. First, the enzyme that catalyzes the amidation reaction (PAM) is subject to tissue-specific and developmentally regulated splicing and expression. Second, the chemistry used for the amidation reaction is distinct from the transamidations used in the formation of other biological amides and is therefore completely dependent on PAM activity. Studies on the regulation of PAM and on the mechanisms of the two sequential reactions catalyzed by PAM are beginning to provide some clues to this important process. The first reaction, the stereospecific α-hydroxylation of the peptide's glycyl extension carried out by PHM, is a particularly interesting reaction, and our structural and mechanistic studies will impact several areas of research. Notably, the reaction involves electron transfer between two distant copper ions and may provide the first example of a substrate-mediated electron-transfer pathway.

Acknowledgments. Support from the National Science Foundation, grant MCB 9982945, and National Institutes of Health, grants DA-00266, DK-32948, DK-32949 and GM-44692, is gratefully acknowledged.

1 Bradbury A. F. and Smyth D. G. (1991) Peptide amidation. Trends Biochem. Sci. **16:** 112–115
2 Patel Y. C. and Galanopoulou A. (1995) Processing and intracellular targeting of prosomatostatin-derived peptides: the role of mammalian endoproteases. Ciba. Found. Symp. **190:** 26–50
3 Lindberg I. and Zhou Y. (1995) Overexpression of neuropeptide precursors and processing enzymes. Methods Neurosci. **23:** 94–108
4 Rouille Y., Duguay S. J., Lund K., Furuta M., Gong Q., Lipkind G. et al. (1995) Proteolytic processing mechanisms in the biosynthesis of neuroendocrine peptides. Front. Neuroendocrinol. **16:** 322–361
5 Yoon J. and Beinfeld M. C. (1997) Prohormone convertase 1 is necessary for the formation of cholecystokinin 8 in Rin5F and STC-1 cells. J. Biol. Chem. **272:** 9450–9456
6 Day R., Lazure C., Basak A., Boudreault A., Limperis P., Dong W. et al. (1998) Prodynorphin processing by proprotein convertase 2. Cleavage at single basic residues and enhanced processing in the presence of carboxypeptidase activity. J. Biol. Chem. **273:** 829–836
7 Seidah N. G., Day R., Marcinkiewicz M. and Chretien M. (1998) Precursor convertases: an evolutionary ancient, cell-specific, combinatorial mechanism yielding diverse bioactive peptides and proteins. Ann. N. Y. Acad. Sci. **839:** 9–24
8 Zhou A., Webb G., Zhu X. and Steiner D. F. (1999) Proteolytic processing in the secretory pathway. J. Biol. Chem. **274:** 20745–20748
9 Cuttitta F. (1993) Peptide amidation: signature of bioactivity. Anat. Rec. **236:** 87–93, 172–173; discussion 193–175
10 Merkler D. J. (1994) C-terminal amidated peptides: production by the in vitro enzymatic amidation of glycine-extended peptides and the importance of the amide to bioactivity. Enzyme Microb. Technol. **16:** 450–456
11 Kolhekar A. S., Roberts M. S., Jiang N., Johnson R. C., Mains R. E., Eipper B. A. et al. (1997) Neuropeptide amidation in *Drosophila*: separate genes encode the two enzymes catalyzing amidation. J. Neurosci. **17:** 1363–1376
12 Eipper B. A., Milgram S. L., Husten E. J., Yun H. Y. and Mains R. E. (1993) Peptidylglycine alpha-amidating monooxygenase: a multifunctional protein with catalytic, processing, and routing domains. Protein Sci. **2:** 489–497
13 Eipper B. A., Quon A. S., Mains R. E., Boswell J. S. and Blackburn N. J. (1995) The catalytic core of peptidylglycine alpha-hydroxylating monooxygenase: investigation by site-directed mutagenesis, Cu X-ray absorption spectroscopy, and electron paramagnetic resonance. Biochemistry **34:** 2857–2865
14 Kulathila R., Merkler K. A. and Merkler D. J. (1999) Enzymatic formation of C-terminal amides. Nat. Prod. Rep. **16:** 145–154
15 Freeman J. C., Villafranca J. J. and Merkler D. J. (1993) Redox cycling of enzyme-bound copper during peptide amidation. J. Am. Chem. Soc. **115:** 4923–4924
16 May V., Mains R. E. and Eipper B. A. (1989) Ability of cofactors to support peptide amidation is cell-type specific. Horm. Res. **32:** 18–21
17 Murthy A. S., Keutmann H. T. and Eipper B. A. (1987) Further characterization of peptidylglycine alpha-amidating monooxygenase from bovine neurointermediate pituitary. Mol. Endocrinol. **1:** 290–299
18 Kolhekar A. S., Mains R. E. and Eipper B. A. (1997) Peptidylglycine alpha-amidating monooxygenase: an ascorbate-requiring enzyme. Methods Enzymol. **279:** 35–43
19 May V. and Eipper B. A. (1985) Regulation of peptide amidation in cultured pituitary cells. J. Biol. Chem. **260:** 16224–16231
20 Mains R. E., Myers A. C. and Eipper B. A. (1985) Hormonal, drug and dietary factors affecting peptidyl glycine alpha-amidating monooxygenase activity in various tissues of the adult male rat. Endocrinology **116:** 2505–2515
21 Li C., Oldham C. D. and May S. W. (1994) NN-dimethyl-1,4-phenylenediamine as an alternative reductant for peptidylglycine alpha-amidating mono-oxygenase catalysis. Biochem J. **300:** 31–36
22 Bell J., Ash D. E., Snyder L. M., Kulathila R., Blackburn N. J. and Merkler D. J. (1997) Structural and functional investigations on the role of zinc in bifunctional rat peptidylglycine alpha-amidating enzyme. Biochemistry **36:** 16239–16246
23 Eipper B. A., Stoffers D. A. and Mains R. E. (1992) The biosynthesis of neuropeptides: peptide alpha-amidation. Annu. Rev. Neurosci. **15:** 57–85
24 Leviev I., Williamson M. and Grimmelikhuijzen C. J. (1997) Molecular cloning of a preprohormone from *Hydra magnipapillata* containing multiple copies of Hydra-L Wamide (Leu-Trp-NH2) neuropeptides: evidence for processing at Ser and Asn residues. J. Neurochem. **68:** 1319–1325

25 Maule A. G., Bowman J. W., Thompson D. P., Marks N. J., Friedman A. R. and Geary T. G. (1996) FMRFamide-related peptides (FaRPs) in nematodes: occurrence and neuromuscular physiology. Parasitology **113:** S119–135

26 Takahashi T., Muneoka Y., Lohmann J., Lopez de Haro M. S., Solleder G., Bosch T. C. et al. (1997) Systematic isolation of peptide signal molecules regulating development in *Hydra*: LWamide and PW families. Proc. Natl. Acad. Sci. USA **94:** 1241–1246

27 Destoumieux D., Bulet P., Loew D., Van Dorsselaer A., Rodriguez J. and Bachere E. (1997) Penaeidins, a new family of antimicrobial peptides isolated from the shrimp *Penaeus vannamei* (Decapoda). J. Biol. Chem. **272:** 28398–28406

28 Lackey D. B. (1992) Isolation and structural determination of a novel TRH-like tripeptide, pyroGlu-Tyr-Pro amide, from alfalfa. J. Biol. Chem. **267:** 17508–17511

29 Gigoux V., Escrieut C., Fehrentz J. A., Poirot S., Maigret B., Moroder L. et al. (1999) Arginine 336 and asparagine 333 of the human cholecystokinin-A receptor binding site interact with the penultimate aspartic acid and the C-terminal amide of cholecystokinin. J. Biol. Chem. **274:** 20457–20464

30 Edison A. S., Espinoza E. and Zachariah C. (1999) Conformational ensembles: the role of neuropeptide structures in receptor binding. J. Neurosci. **19:** 6318–6326

31 Bignon E., Alonso R., Arnone M., Boigegrain R., Brodin R., Gueudet C. et al. (1999) SR146131: a new potent, orally active and selective nonpeptide cholecystokinin subtype 1 receptor agonist. II. In vivo pharmacological characterization. J. Pharmacol. Exp. Ther. **289:** 752–761

32 Lingueglia E., Champigny G., Lazdunski M. and Barbry P. (1995) Cloning of the amiloride-sensitive FMRFamide peptide-gated sodium channel. Nature **378:** 730–733

33 Kumar A. M., Agarwal R. K., Thompson M. L., Marchand J. E., Kream R. M. and Engelking L. R. (1994) Effect of chronic DDC treatment on LHRH and substance P amidation processes in the rat. Brain Res. Bull. **33:** 337–344

34 Kaise M., Muraoka A., Seva C., Takeda H., Dickinson C. J. and Yamada T. (1995) Glycine-extended progastrin processing intermediates induce H+, K(+)-ATPase alpha-subunit gene expression through a novel receptor. J. Biol. Chem. **270:** 11155–11160

35 Dockray G. J., Varro A. and Dimaline R. (1996) Gastric endocrine cells: gene expression, processing, and targeting of active products. Physiol. Rev. **76:** 767–798

36 Kapuscinski M., Green M., Sinha S. N., Shepherd J. J. and Shulkes A. (1993) Peptide alpha-amidation activity in human plasma: relationship to gastrin processing. Clin. Endocrinol. **39:** 51–58

37 Kitamura K., Kato J., Kawamoto M., Tanaka M., Chino N., Kangawa K. et al. (1998) The intermediate form of glycine-extended adrenomedullin is the major circulating molecular form in human plasma. Biochem. Biophys. Res. Commun. **244:** 551–555

38 Amico J. A. and Hempel J. (1990) An oxytocin precursor intermediate circulates in the plasma of humans and rhesus monkeys administered estrogen. Neuroendocrinology **51:** 437–443

39 Seva C., Dickinson C. J. and Yamada T. (1994) Growth-promoting effects of glycine-extended progastrin. Science **265:** 410–412

40 Todisco A., Takeuchi Y., Seva C., Dickinson C. J. and Yamada T. (1995) Gastrin and glycine-extended progastrin processing intermediates induce different programs of early gene activation. J. Biol. Chem. **270:** 28337–28341

41 Grimmelikhuijzen C. J. P., Darmer D., Schmutzler C., Reinscheid R. K. and Carstensen K. (1994) Biosynthesis of neuropeptides in the *Cnidaria*: new discoveries of old principles. Perspectives Comp. Endocrinol. 97–108

42 Mitgutsch C., Hauser F. and Grimmelikhuijzen C. J. P. (1999) Expression and developmental regulation of the hydra-RFamide and hydra-LWamide preprohormone genes in *Hydra*: evidence for transient phases of head formation. Dev. Biol. **207:** 189–203

43 Schmich J., Trepel S. and Leitz T. (1998) The role of GLWamides in metamorphosis of *Hydractinia echinata*. Dev. Genes Evol. **208:** 267–273

44 Xin Y., Hurwitz I., Perrins R., Evans C. G., Alexeeva V., Weiss K. R. and Kupfermann I. (1999) Actions of a pair of identified cerebral-buccal interneurons (CBI-8/9) in *Aplysia* that contain the peptide myomodulin. J. Neurophysiol. **81:** 507–520

45 Wang Y., Strong J. A. and Sahley C. L. (1999) Modulatory effects of myomodulin on the excitability and membrane currents in Retzius cells of the leech. J. Neurophysiol. **82:** 216–225

46 Nelson L. S., Rosoff M. L. and Li C. (1998) Disruption of a neuropeptide gene, flp-1, causes multiple behavioral defects in *Caenorhabditis elegans*. Science **281:** 1686–1690

47 Martinez A., Miller M. J., Unsworth E. J., Siegfried J. M. and Cuttitta F. (1995) Expression of adrenomedullin in normal human lung and in pulmonary tumors. Endocrinology **136:** 4099–4105

48 Eguchi S., Hirata Y., Iwasaki H., Sato K., Watanabe T. X., Inui T. et al. (1994) Structure-activity relationship of adrenomedullin, a novel vasodilatory peptide, in cultured rat vascular smooth muscle cells. Endocrinology **135:** 2454–2458

49 Arimura A., Somogyvari-Vigh A., Weill C., Fiore R. C., Tatsuno I., Bay V. et al. (1994) PACAP functions as a neurotrophic factor. Ann. N.Y. Acad. Sci. **739:** 228–243

50 De Felipe C., Pinnock R. D. and Hunt S. P. (1995) Modulation of chemotropism in the developing spinal cord by substance P. Science **267:** 899–902

51 Dickinson C. J., Daugherty D., Guo Y. J., Stadler B., Finniss S. and Yamada T. (1993) Substrate specificity of the gastrin-amidating enzyme. J. Biol. Chem. **268:** 15929–15934

52 Landymore-Lim A. E., Bradbury A. F. and Smyth D. G. (1983) The amidating enzyme in pituitary will accept a peptide with C-terminal D-alanine as substrate. Biochem. Biophys. Res. Commun. **117:** 289–293

53 Katopodis A. G. and May S. W. (1990) Novel substrates and inhibitors of peptidylglycine alpha-amidating monooxygenase. Biochemistry **29:** 4541–4548

54 Merkler D. J., Merkler K. A., Stern W. and Fleming F. F. (1996) Fatty acid amide biosynthesis: a possible new role for peptidylglycine alpha-amidating enzyme and acyl-coenzyme A: glycine N-acyltransferase. Arch. Biochem. Biophys. **330:** 430–434

55 Wilcox B. J., Ritenour-Rodgers K. J., Asser A. S., Baumgart L. E., Baumgart M. A., Boger D. L. et al. (1999) N-acylglycine amidation: implications for the biosynthesis of fatty acid primary amides. Biochemistry **38:** 3235–3245

56 Merkler D. J., Glufke U., Ritenour-Rodgers K. J., Baumgart L. E., DeBlassio J. L., Merkler K. A. et al. (1999) Formation of nicotinamide from nicotinuric acid by peptidylglycine alpha-amidating monooxygenase (PAM): a possible alternative route from nicotinic acid (niacin) to NADP in mammals. J. Am. Chem. Soc. **121:** 4904–4905

57 Cravatt B. F., Prospero-Garcia O., Siuzdak G., Gilula N. B., Henriksen S. J., Boger D. L. et al. (1995) Chemical characterization of a family of brain lipids that induce sleep. Science **268:** 1506–1509

58 Boger D. L., Patterson J. E., Guan X., Cravatt B. F., Lerner R. A. and Gilula N. B. (1998) Chemical requirements for inhibition of gap junction communication by the biologically active lipid oleamide. Proc. Natl. Acad. Sci. USA **95:** 4810–4815

59 Oldham C. D., Li C., Girard P. R., Nerem R. M. and May S. W. (1992) Peptide amidating enzymes are present in cultured endothelial cells. Biochem. Biophys. Res. Commun. **184:** 323–329

60 Saldise L., Martinez A., Montuenga L. M., Treston A., Springall D. R., Polak J. M. et al. (1996) Distribution of

peptidyl-glycine alpha-amidating mono-oxygenase (PAM) enzymes in normal human lung and in lung epithelial tumors. J. Histochem. Cytochem. **44:** 3–12
61 Ogonowski A. A., May S. W., Moore A. B., Barrett L. T., O'Bryant C. L. and Pollock S. H. (1997) Antiinflammatory and analgesic activity of an inhibitor of neuropeptide amidation. J. Pharmacol. Exp. Ther. **280:** 846–853
62 Klein R. S. and Fricker L. D. (1992) Heterogeneous expression of carboxypeptidase E and proenkephalin mRNAs by cultured astrocytes. Brain Res. **569:** 300–310
63 Jaworsky D. E., Eipper B. A. and Ronnett G. V. (1999) Expression of PAM and amidated neuropeptides in developing and adult rat olfactory epithelium. Soc. Neurosci. 29th Ann. Mtg. Abst. 428.10
64 Zhang J., Zheng M., Eipper B. A. and Pintar J. E. (1997) Embryonic and uterine expression patterns of peptidylglycine alpha-amidating monooxygenase transcripts suggest a widespread role for amidated peptides in development. Dev. Biol. **192:** 375–391
65 Martinez A. and Treston A. M. (1996) Where does amidation take place? Mol. Cell. Endocrinol. **123:** 113–117
66 Scopsi L., Lee R., Gullo M., Collini P., Husten E. J. and Eipper B. A. (1998) Peptidylglycine alpha-amidating monooxygenase in neuroendocrine tumors. Appl. Immunohistochem. **6:** 120–132
67 Siegfried J. M., Han Y.-H., DeMichele M. A., Hunt J. D., Gaither A. L. and Cuttitta F. (1994) Production of gastrin-releasing peptide by a non-small cell lung carcinoma cell line adapted to serum-free and growth factor-free conditions. J. Biol. Chem. **269:** 8596–8603
68 Iwai N., Martinez A., Miller M. J., Vos M., Mulshine J. L. and Treston A. M. (1999) Autocrine growth loops dependent on peptidyl alpha-amidating enzyme as targets for novel tumor cell growth inhibitors. Lung Cancer **23:** 209–222
69 Oyarce A. M., Hand T. A., Mains R. E. and Eipper B. A. (1996) Dopaminergic regulation of secretory granule-associated proteins in rat intermediate pituitary. J. Neurochem. **67:** 229–241
70 Grino M., Guillaume V., Boudouresque F., Conte-Devolx B., Maltese J. Y. and Oliver C. (1990) Glucocorticoids regulate peptidyl-glycine alpha-amidating monooxygenase gene expression in the rat hypothalamic paraventricular nucleus. Mol. Endocrinol. **4:** 1613–1619
71 El Meskini R., Delfino C., Boudouresque F., Hery M., Oliver C. and Ouafik L. (1997) Estrogen regulation of peptidylglycine alpha-amidating monooxygenase expression in anterior pituitary gland. Endocrinology **138:** 379–388
72 El Meskini R., Delfino C., Boudouresque F., Oliver C., Martin P. M. and Ouafik L. H. (1998) Evidence of high expression of peptidylglycine alpha-amidating monooxygenase in the rat uterus: estrogen regulation. Proc. Natl. Acad. Sci. USA **95:** 7191–7196
73 Mueller G. P., Husten E. J., Mains R. E. and Eipper B. A. (1993) Peptide alpha-amidation and peptidylglycine alpha-hydroxylating monooxygenase: control by disulfiram. Mol. Pharmacol. **44:** 972–980
74 Driscoll W. J., Mueller S. A., Eipper B. A. and Mueller G. P. (1999) Differential regulation of peptide alpha-amidation by dexamethasone and disulfiram. Mol. Pharmacol. **55:** 1067–1076
75 Zabriskie T. M., Cheng H. and Vederas J. C. (1992) Mechanism-based inactivation of peptidylglycine alpha-hydroxylating monooxygenase (PHM) by a substrate analogue, D-phenylalanyl-L-phenylalanyl-D-vinylglycine: inhibition of formation of peptide C-terminal amides. J. Am. Chem. Soc. **114:** 2270–2272
76 Mueller G. P., Driscoll W. J. and Eipper B. A. (1999) In vivo inhibition of peptidylglycine-alpha-hydroxylating monooxygenase by 4-phenyl-3-butenoic acid. J. Pharmacol. Exp. Ther. **290:** 1331–1336
77 Bolkenius F. N., Ganzhorn A. J., Chanal M. C. and Danzin C. (1997) Selective mechanism-based inactivation of peptidylglycine alpha-hydroxylating monooxygenase in serum and heart atrium vs. brain. Biochem. Pharmacol. **53:** 1695–1702
78 Merkler D. J., Kulathila R. and Ash D. E. (1995) The inactivation of bifunctional peptidylglycine alpha-amidating enzyme by benzylhydrazine: evidence that the two enzyme-bound copper atoms are nonequivalent. Arch. Biochem. Biophys. **317:** 93–102
79 Moore A. B. and May S. W. (1999) Kinetic and inhibition studies on substrate channeling in the bifunctional enzyme catalyzing C-terminal amidation. Biochem. J. **341:** 33–40
80 Jeng A. Y., Fujimoto R. A., Chou M., Tan J. and Erion M. D. (1997) Suppression of substance P biosynthesis in sensory neurons of dorsal root ganglion by prodrug esters of potent peptidylglycine alpha-amidating monooxygenase inhibitors. J. Biol. Chem. **272:** 14666–14671
81 Erion M. D., Tan J., Wong M. and Jeng A. Y. (1994) Inhibition of peptidylglycine alpha-amidating monooxygenase by N-substituted homocysteine analogs. J. Med. Chem. **37:** 4430–4437
82 Mounier C. E., Shi J., Sirimanne S. R., Chen B. H., Moore A. B., Gill-Woznichak M. M. et al. (1997) Pyruvate-extended amino acid derivatives as highly potent inhibitors of carboxyl-terminal peptide amidation. J. Biol. Chem. **272:** 5016–5023
83 Guembe L., Villaro A. C. and Treston A. M. (1999) Immunocytochemical mapping of the amidating enzyme PAM in the developing and adult mouse lung. J. Histochem. Cytochem. **47:** 623–636
84 Fenger M. and Hilsted L. (1988) Influence of ascorbic acid on in vivo amidation of alpha-melanocyte stimulating hormone in guinea pig pituitary. Acta. Endocrinol. **118:** 119–124
85 Marchand J. E., Shimonaka H. and Kream R. M. (1991) Biochemical characterization and anatomical distribution of a major form of unamidated precursor of substance P in rat brain. Brain Res. **567:** 290–305
86 Tsukaguchi H., Tokui T., Mackenzie B., Berger U. V., Chen X. Z., Wang Y. et al. (1999) A family of mammalian Na + -dependent L-ascorbic acid transporters. Nature **399:** 70–75
87 Hamman B. D., Hendershot L. M. and Johnson A. E. (1998) BiP maintains the permeability barrier of the ER membrane by sealing the lumenal end of the translocon pore before and early in translocation. Cell **92:** 747–758
88 Matlack K. E., Misselwitz B., Plath K. and Rapoport T. A. (1999) BiP acts as a molecular ratchet during posttranslational transport of prepro-alpha factor across the ER membrane. Cell **97:** 553–564
89 Fleming P. J. and Kent U. M. (1991) Cytochrome b561, ascorbic acid, and transmembrane electron transfer. Am. J. Clin. Nutr. **54:** 1173S–1178S
90 Njus D. and Kelley P. M. (1993) The secretory-vesicle ascorbate-regenerating system: a chain of concerted H + / e(−)-transfer reactions. Biochim. Biophys. Acta. **1144:** 235–248
91 Ingebretsen O. C., Terland O. and Flatmark T. (1980) Subcellular distribution of ascorbate in bovine adrenal medulla. Evidence for accumulation in chromaffin granules against a concentration gradient. Biochim. Biophys. Acta **628:** 182–189
92 Srivastava M. (1995) Genomic structure and expression of the human gene encoding cytochrome b561, an integral protein of the chromaffin granule membrane. J. Biol. Chem. **270:** 22714–22720
93 Prigge S. T., Kolhekar A. S., Eipper B. A., Mains R. E. and Amzel L. M. (1999) Substrate-mediated electron transfer in peptidylglycine alpha-hydroxylating monooxygenase. Nat. Struct. Biol. **6:** 976–983
94 Harris Z. L. and Gitlin J. D. (1996) Genetic and molecular basis for copper toxicity. Am. J. Clin. Nutr. **63:** 836S–841S
95 Mercer J. F. (1998) Menkes syndrome and animal models. Am. J. Clin. Nutr. **67:** 1022S–1028S

96 Petris M. J., Mercer J. F., Culvenor J. G., Lockhart P., Gleeson P. A. and Camakaris J. (1996) Ligand-regulated transport of the Menkes copper P-type ATPase efflux pump from the Golgi apparatus to the plasma membrane: a novel mechanism of regulated trafficking. EMBO J. **15:** 6084–6095

97 Turner Z. and Horn N. (1997) Menkes disease: recent advances and new aspects. J. Med. Genet. **34:** 265–274

98 Yamaguchi Y., Heiny M. E., Suzuki M. and Gitlin J. D. (1996) Biochemical characterization and intracellular localization of the Menkes disease protein. Proc. Natl. Acad. Sci. USA **93:** 14030–14035

99 Prohaska J. R., Tamura T., Percy A. K. and Turnlund J. R. (1997) In vitro copper stimulation of plasma peptidylglycine alpha-amidating monooxygenase in Menkes disease variant with occipital horns. Pediatr. Res. **42:** 862–865

100 Pufahl R. A., Singer C. P., Peariso K. L., Lin S.-J., Schmidt P. J., Fahrni C. J. et al. (1997) Metal ion chaperone function of the soluble Cu(I) receptor Atx1. Science **278:** 853–856

101 Koch K. A., Pena M. M. and Thiele D. J. (1997) Copper-binding motifs in catalysis, transport, detoxification and signaling. Chem. Biol. **4:** 549–560

102 Culotta V. C., Klomp L. W., Strain J., Casareno R. L., Krems B. and Gitlin J. D. (1997) The copper chaperone for superoxide dismutase. J. Biol. Chem. **272:** 23469–23472

103 Larin D., Mekios C., Das K., Ross B., Yang A. S. and Gilliam T. C. (1999) Characterization of the interaction between the Wilson and Menkes disease proteins and the cytoplasmic copper chaperone, HAH1p. J. Biol. Chem. **274:** 28497–28504

104 Yun H. Y. and Eipper B. A. (1995) Addition of an endoplasmic reticulum retention/retrieval signal does not block maturation of enzymatically active peptidylglycine alpha-amidating monooxygenase. J. Biol. Chem. **270:** 15412–15416

105 Arvan P. and Castle D. (1998) Sorting and storage during secretory granule biogenesis: looking backward and looking forward. Biochem J. **332:** 593–610

106 Urbe S., Tooze S. A. and Barr F. A. (1997) Formation of secretory vesicles in the biosynthetic pathway. Biochim. Biophys. Acta **1358:** 6–22

107 Bauerfeind R., Galli T. and De Camilli P. (1996) Molecular mechanisms in synaptic vesicle recycling. J. Neurocytol. **25:** 701–715

108 Dannies P. S. (1999) Protein hormone storage in secretory granules: mechanisms for concentration and sorting. Endocr. Rev. **20:** 3–21

109 Thiele C., Gerdes H. H. and Huttner W.B. (1997) Protein secretion: puzzling receptors. Curr. Biol. **7:** R496–R500

110 Milgram S. L., Eipper B. A. and Mains R. E. (1994) Differential trafficking of soluble and integral membrane secretory granule-associated proteins. J. Cell Biol. **124:** 33–41

111 Milgram S. L., Kho S. T., Martin G. V., Mains R. E. and Eipper B. A. (1997) Localization of integral membrane peptidylglycine alpha-amidating monooxygenase in neuroendocrine cells. J. Cell Sci. **110:** 695–706

112 Alam M. R., Johnson R. C., Darlington D. N., Hand T. A., Mains R. E. and Eipper B. A. (1997) Kalirin, a cytosolic protein with spectrin-like and GDP/GTP exchange factor-like domains that interacts with peptidylglycine alpha-amidating monooxygenase, an integral membrane peptide-processing enzyme. J. Biol. Chem. **272:** 12667–12675

113 Wulff B. S., Catipovic B., Okamoto H., Gether U., Schwartz T. W. and Johansen T. E. (1993) Efficient amidation of C-peptide deleted NPY precursors by non-endocrine cells is affected by the presence of Lys-Arg at the C-terminus. Mol. Cell. Endocrinol. **91:** 135–141

114 Takahashi K. I., Liu Y. C., Hayashi N., Goto F., Kato M., Kawashima H. et al. (1997) Production of bioactive salmon calcitonin from the nonendocrine cell lines COS-7 and CHO. Peptides **18:** 439–444

115 McKee C., Gibson A., Dalrymple M., Emslie L., Garner I. and Cottingham I. (1998) Production of biologically active salmon calcitonin in the milk of transgenic rabbits. Nat. Biotechnol. **16:** 647–651

116 Eipper B. A., Green C. B., Campbell T. A., Stoffers D. A., Keutmann H. T., Mains R. E. et al. (1992) Alternative splicing and endoproteolytic processing generate tissue-specific forms of pituitary peptidylglycine alpha-amidating monooxygenase (PAM). J. Biol. Chem. **267:** 4008–4015

117 Stoffers D. A., Ouafik L. and Eipper B. A. (1991) Characterization of novel mRNAs encoding enzymes involved in peptide alpha-amidation. J. Biol. Chem. **266:** 1701–1707

118 Ouafik L. H., Stoffers D. A., Campbell T. A., Johnson R. C., Bloomquist B. T., Mains R. E. et al. (1992) The multifunctional peptidylglycine alpha-amidating monooxygenase gene: exon/intron organization of catalytic, processing and routing domains. Mol. Endocrinol. **6:** 1571–1584

119 Glauder J., Ragg H., Rauch J. and Engels J. W. (1990) Human peptidylglycine alpha-amidating monooxygenase: cDNA, cloning and functional expression of a truncated form in COS cells. Biochem. Biophys. Res. Commun. **169:** 551–558

120 Vos M. D., Jones J. E. and Treston A. M. (1995) Human peptidylglycine alpha-amidating monooxygenase transcripts derived by alternative mRNA splicing of an unreported exon. Gene **163:** 307–311

121 Husten E. J., Tausk F. A., Keutmann H. T. and Eipper B. A. (1993) Use of endoproteases to identify catalytic domains, linker regions, and functional interactions in soluble peptidylglycine alpha-amidating monooxygenase. J. Biol. Chem. **268:** 9709–9717

122 Husten E. J. and Eipper B. A. (1991) The membrane-bound bifunctional peptidylglycine alpha-amidating monooxygenase protein. Exploration of its domain structure through limited proteolysis. J. Biol. Chem. **266:** 17004–17010

123 Kolhekar A. S., Keutmann H. T., Mains R. E., Quon A. S. W. and Eipper B. A. (1997) Peptidylglycine alpha-hydroxylating monooxygenase: active site residues, disulfide linkages, and a two-domain model of the catalytic core. Biochemistry **36:** 10901–10909

124 Kolhekar A. S., Quon A. S., Berard C. A., Mains R. E. and Eipper B. A. (1998) Post-translational N-glycosylation of a truncated form of a peptide processing enzyme. J. Biol. Chem. **273:** 23012–23018

125 Iwasaki Y., Shimoi H., Saiki H. and Nishikawa Y. (1993) Tissue-specific molecular diversity of amidating enzymes (peptidylglycine alpha-hydroxylating monooxygenase and peptidylhydroxyglycine N-C lyase) in *Xenopus laevis*. Eur. J. Biochem. **214:** 811–818

126 Spijker S., Smit A. B., Eipper B. A., Malik A., Mains R. E. and Geraerts W. P. (1999) A molluscan peptide alpha-amidating enzyme precursor that generates five distinct enzymes. FASEB J. **13:** 735–748

127 Hauser F., Williamson M. and Grimmelikhuijzen C. J. (1997) Molecular cloning of a peptidylglycine alpha-hydroxylating monooxygenase from sea anemones. Biochem. Biophys. Res. Commun. **241:** 509–512

128 Kim H., Kelly R. E. and Evans D. R. (1992) The structural organization of the hamster multifunctional protein CAD. Controlled proteolysis, domains and linkers. J. Biol. Chem. **267:** 7177–7184

129 Guy H. I. and Evans D. R. (1994) Cloning and expression of the mammalian multifunctional protein CAD in *Escherichia coli*. Characterization of the recombinant protein and a deletion mutant lacking the major interdomain linker. J. Biol. Chem. **269:** 23808–23816

130 Green J. D., Perham R. N., Ullrich S. J. and Appella E. (1992) Conformational studies of the interdomain linker peptides in the dihydrolipoyl acetyltransferase component of the pyruvate dehydrogenase multienzyme complex of *Escherichia coli*. J. Biol. Chem. **267:** 23484–23488

131 Southan C. and Kruse L. I. (1989) Sequence similarity between dopamine beta-hydroxylase and peptide alpha-amidating enzyme: evidence for a conserved catalytic domain. FEBS Lett. **255:** 116–120

132 Robertson J. G., Adams G. W., Medzihradszky K. F., Burlingame A. L. and Villafranca J. J. (1994) Complete assignment of disulfide bonds in bovine dopamine beta-hydroxylase. Biochemistry **33:** 11563–11575
133 Kobayashi K., Kurosawa Y., Fujita K. and Nagatsu T. (1989) Human dopamine beta-hydroxylase gene: two mRNA types having different 3′-terminal regions are produced through alternative polyadenylation. Nucleic Acids Res. **17:** 1089–1102
134 Chambers K. J., Tonkin L. A., Chang E., Shelton D. N., Linskens M. H. and Funk W. D. (1998) Identification and cloning of a sequence homologue of dopamine beta-hydroxylase. Gene **218:** 111–120
135 Monastirioti M., Linn C. E. Jr and White K. (1996) Characterization of *Drosophila* tyramine beta-hydroxylase gene and isolation of mutant flies lacking octopamine. J. Neurosci. **16:** 3900–3911
136 Prigge S. T., Kolhekar A. S., Eipper B. A., Mains R. E. and Amzel L. M. (1997) Amidation of bioactive peptides: the structure of peptidylglycine alpha-hydroxylating monooxygenase. Science **278:** 1300–1305
137 Holm L. and Sander C. (1993) Protein structure comparison by alignment of distance matrices. J. Mol. Biol. **233:** 123–138
138 Reedy B. J. and Blackburn N. J. (1994) Preparation and characterization of half-apo dopamine beta-hydroxylase by selective removal of CuA. Identification of a sulfur ligand at the dioxygen binding site by EXAFS and FITR spectroscopy. J. Am. Chem. Soc. **116:** 1924–1931
139 Boswell J. S., Reedy B. J., Kulathila R., Merkler D. and Blackburn N. J. (1996) Structural investigations on the coordination environment of the active-site copper centers of recombinant bifunctional peptidylglycine alpha-amidating enzyme. Biochemistry **35:** 12241–12250
140 Blackburn N. J., Hasnain S. S., Pettingill T. M. and Strange R. W. (1991) Copper K-extended x-ray absorption fine structure studies of oxidized and reduced dopamine beta-hydroxylase. Confirmation of a sulfur ligand to copper(I) in the reduced enzyme. J. Biol. Chem. **266:** 23120–23127
141 Blackburn N. J., Pettingill T. M., Seagraves K. S. and Shigeta R. T. (1990) Characterization of a carbon monoxide complex of reduced dopamine beta-hydroxylase. Evidence for inequivalence of the Cu(I) centers. J. Biol. Chem. **265:** 15383–15386
142 Pettingill T. M., Strange R. W. and Blackburn N. J. (1991) Carbonmonoxy dopamine beta-hydroxylase. Structural characterization by Fourier transform infrared, fluorescence and x-ray absorption spectroscopy. J. Biol. Chem. **266:** 16996–17003
143 Yonekura H., Anzai T., Kato I., Furuya Y., Shizuta S., Takasawa S. et al. (1996) Identification of the five essential histidine residues for peptidylglycine monooxygenase. Biochem. Biophys. Res. Commun. **218:** 495–499
144 Ramer S. E., Cheng H., Palcic M. M. and Vederas J. C. (1988) Formation of peptide amides by peptidylglycine alpha-amidating monooxygenase: a new assay and stereochemistry of hydrogen loss. J. Am. Chem. Soc. **110:** 8526–8532
145 Francisco W. A., Merkler D. J., Blackburn N. J. and Klinman J. P. (1998) Kinetic mechanism and intrinsic isotope effects for the peptidylglycine alpha-amidating enzyme reaction. Biochemistry **37:** 8244–8252
146 Brenner M. C. and Klinman J. P. (1989) Correlation of copper valency with product formation in single turnovers of dopamine beta-monooxygenase. Biochemistry **28:** 4664–4670
147 Fitzpatrick P. F. and Villafranca J. J. (1986) The mechanism of inactivation of dopamine beta-hydroxylase by hydrazines. J. Biol. Chem. **261:** 4510–4518
148 Battersby A. R., Sheldrake P. W., Staunton J. and Williams D. C. (1976) Studies of enzyme-mediated reactions. Part VII. Stereospecific syntheses of tritium-labelled (2*R*)- and (2*S*)-dopamines: stereochemical course of hydroxylation of dopamine by dopamine beta-hydroxylase (E.C. 1.14.17.1). J. Chem. Soc. [Perkin 1]: 1056–1062
149 Bradbury A. F., Mistry J., Roos B. A. and Smyth D. G. (1990) 4-Phenyl-3-butenoic acid, an in vivo inhibitor of peptidylglycine hydroxylase (peptide amidating enzyme). Eur. J. Biochem. **189:** 363–368
150 Ping D., Katopodis A. G. and May S. W. (1992) Tandem stereochemistry of peptidylglycine alpha-monooxygenase and petidylamidoglycolate lyase, the two enzymes involved in peptide amidation. J. Am. Chem. Soc. **114:** 3998–4000
151 Zabriskie T. M., Cheng H. and Vederas J. C. (1991) Incorporation of oxygen into the hydroxyglycyl intermediate during formation of C-terminal peptide amides by peptidylglycine alpha-amidating monooxygenase (PAM). J. Chem. Soc. [Chem. Commun.] 571–572
152 Merkler D. J., Kulathila R., Consalvo A. P., Young S. D. and Ash D. E. (1992) ^{18}O isotopic ^{13}C NMR shift as proof that bifunctional peptidylglycine alpha-amidating enzyme is a monooxygenase. Biochemistry **31:** 7282–7288
153 Noguchi M., Seino H., Kochi H., Okamoto H., Tanaka T. and Hirama M. (1992) The source of the oxygen atom in the alpha-hydroxyglycine intermediate of the peptidylglycine alpha-amidating reaction. Biochem. J. **283:** 883–888
154 Tian G., Berry J. A. and Klinman J. P. (1994) Oxygen-18 kinetic isotope effects in the dopamine beta-monooxygenase reaction: evidence for a new chemical mechanism in non-heme metallomonooxygenases. Biochemistry **33:** 226–234
155 Ahn N. and Klinman J. P. (1983) Mechanism of modulation of dopamine beta-monooxygenase by pH and fumarate as deduced from initial rate and primary deuterium isotope effect studies. Biochemistry **22:** 3096–3106
156 Pedersen J. Z. and Finazzi-Agro A. (1991) Protein-radical enzymes. FEBS Lett. **325:** 53–58
157 Beratan D. N., Betts J. N. and Onuchic J. N. (1991) Protein electron transfer rates set by the bridging secondary and tertiary structure. Science **252:** 1285–1288
158 Beratan D. and Skourtis S. (1998) Electron transfer mechanisms. Curr. Opin. Chem. Biol. **2:** 235–243
159 Rhodes C. H. and Honsinger C. (1993) Structure-activity relationships among inhibitors of peptidylglycine amidating monooxygenase. Ann. N.Y. Acad. Sci. **689:** 663–666
160 Casara P., Ganzhorn A., Philippo C., Chanal M.-C. and Danzin C. (1996) Unsaturated thioacetic acids as novel mechanism-based inhibitors of peptidylglycine alpha-hydroxylating monooxygenase. Bioorg. Med. Chem. Let. **6:** 393–396
161 Karlin K. D., Kaderli S. and Zuberbuhler A. D. (1997) Kinetic and thermodynamics of copper(I)/dioxygen interaction. Acc. Chem. Res. **30:** 139–147
162 Casella L. and Gullotti M. (1993) Dioxygen activation by biomimetic dinuclear complexes. In: Bioinorganic Chemistry of Copper, pp. 292–305, Karlin K. D. and Tyeklar Z. (eds), Chapman and Hall, New York
163 Casella L., Gullotti M., Bartosek M., Pallanza G. and Laurenti E. (1991) Model monooxygenase reactivity by binuclear two-coordinate copper(I) complexes extends to new ligand systems containing nitrogen and sulfur donors. J. Chem. Soc. [Chem. Commun.] 1235–1237
164 Bernhard P. and Anson F.C. (1988) Hydrogen abstraction from amine complexes of Iron(II), Cobalt(II), and Rutheniu-m(II) by superoxide. Influence of driving force on rate. Inorg. Chem. **27:** 4574–4577
165 Hurley T. D., Bosron W. F., Stone C. L. and Amzel L. M. (1994) Structures of three human beta alcohol dehydrogenase variants. Correlations with their functional differences. J. Mol. Biol. **239:** 415–429
166 Wimalasena K. and Wimalasena D. S. (1995) The reduction of membrane-bound dopamine beta-monooxygenase in re-sealed chromaffin granule ghosts. Is intragranular ascorbic acid a mediator for extragranular reducing equivalents? J. Biol. Chem. **270:** 27516–27524

167 Evans S. V. (1993) Hardware-lighted three-dimensional solid model representations of macromolecules. J. Mol. Graph. **11:** 134–136
168 Miller S. M. and Klinman J. P. (1985) Secondary isotope effects and structure-reactivity correlations in the dopamine beta-monooxygenase reaction: evidence for a chemical mechanism. Biochemistry **24:** 2114–2127
169 Harata M., Jitsukawa K., Masuda H. and Einaga H. (1994) A structurally characterized mononuclear copper(II)-superoxo complex. J. Am. Chem. Soc. **116:** 10817–10818